

Modeling and Validation of BADA 4 Piston Aircraft Performance

Papoči, Petar

Master's thesis / Diplomski rad

2020

Degree Grantor / Ustanova koja je dodijelila akademski / stručni stupanj: **University of Zagreb, Faculty of Transport and Traffic Sciences / Sveučilište u Zagrebu, Fakultet prometnih znanosti**

Permanent link / Trajna poveznica: <https://urn.nsk.hr/urn:nbn:hr:119:944678>

Rights / Prava: [In copyright](#)/[Zaštićeno autorskim pravom.](#)

Download date / Datum preuzimanja: **2024-08-06**



Repository / Repozitorij:

[Faculty of Transport and Traffic Sciences - Institutional Repository](#)



UNIVERSITY OF ZAGREB
FACULTY OF TRANSPORT AND TRAFFIC SCIENCES

Petar Papoči

**MODELLING AND VALIDATION OF BADA 4 AIRCRAFT PISTON
PERFORMANCE**

GRADUATE THESIS

Zagreb, 2020

Zagreb, 6 April 2020

MASTER THESIS ASSIGNMENT No. 5656

Student: **Petar Papoči (0135240528)**
Study: Aeronautics

Title: **Modeling and Validation of BADA 4 Aircraft Piston Performance**

Description:

BADA (Base of Aircraft Data) is the aircraft performance model, managed by EUROCONTROL for use by the aviation community. The main application of BADA is trajectory simulation and prediction. The purpose of this diploma thesis is to familiarise with the BADA modelling process and existing model specifications for BADA 4 piston model. The student tasks are:

- the review of the BADA theoretical model and validation based on the existing aircraft/engine/propeller performance reference data.
- Identification of the areas of improvement in the BADA theoretical model and/or modelling process, in order to increase the accuracy of the model.
- Preliminary ideas for modifications in the model specification implementation supported by prototyping implementations and validation.

Mentor:

Committee Chair:

Assistant Professor Karolina Krajček
Nikolić, PhD

University of Zagreb
Faculty of transport and traffic sciences

GRADUATE THESIS

**MODELLING AND VALIDATION OF BADA 4 AIRCRAFT PISTON
PERFORMANCE**

Modeliranje i validacija performansi BADA 4 elisno klipnog
pogonskog sustava

Supervisor: doc. dr. sc. Karolina Krajček Nikolić

Student: Petar Papoči

JMBAG: 0135240528

Zagreb, 2020

Preface

This paper is depicted as graduate thesis and rounds up some knowledge and skills acquired during the studies.

Great opportunity is one, where one gets to both learn and achieve something. This Eurocontrol traineeship is a perfect example of this. Throughout the whole duration of traineeship, five months in total, from 1st April to 31st August, I learned at least one new thing every day, and to work with such amazing people in general is the biggest opportunity one can be offered.

I want to express my gratitude to Angela Nuić, project manager on BADA in Eurocontrol, who made this traineeship possible with extraordinary efforts, and for hers continuous support throughout the traineeship period.

I also want to thank Vincent Mouillet, aircraft performance modelling expert in Eurocontrol, who played the Eurocontrol mentor role throughout the traineeship. As well, for his immense patience and will to guide me throughout this traineeship.

It is also required to thank the Henrich Glaser-Opitz for his continuous work and assistance during the traineeship, and insight into flight test from another pilot's perspective.

At last, but not least, I want to express gratitude to my mentor Karolina Krajček Nikolić, who helped me a lot not only during the traineeship period but throughout whole university studies. She was of constant support and an idol for whom the problems simply don't exist.

Petar Papoči

Summary

Increasing trend of air traffic leads to the congested airspace and overwhelmed air navigation service providers. New procedures and technology are implemented every day, but with rigorous testing. Simulations are a part of that testing, but every simulation is as good as its model. Within the traineeship in Eurocontrol, the current Base of Aircraft Data Family 4 (BADA 4) is analysed and searched for the possible improvements in the segment of the piston propeller powered aircraft. The model for these aircraft isn't as good as it could be, and at this point it is necessary to improve it due to the fact that the number of general aviation aircraft (mostly piston powered) is increasing. During research and validation of the initial model it was determined that some improvements need to take place in engine power modelling alongside with the propeller efficiency modelling. Cruise data as a primary source for drag polar coefficients and vertical speed conversion to the rate of climb were introduced. With all of these corrections, or improvements, correct performance data was reproduced to resemble the performance data published in the aircraft's manual. At a certain point to gain an insight into the published performance data, and to gain some additional data, two flight tests took place. As a result of flight tests, the published data was confirmed throughout usage of different data reduction methods. In conclusion, certain improvements were established, and proposed to the Eurocontrol team. Implementation of these improvements into the Eurocontrol BADA 4 tool will be done by Eurocontrol team at a certain point, if they determine that these proposed changes do bring a necessary improvement their model.

Keywords

Eurocontrol, Base of Aircraft Data (BADA), BADA Family 4 (BADA 4), simulation, model, air traffic, airspace, piston engine, propeller, performance, flight test, data reduction methods

Sažetak

Povećanje zračnog prometa i trend porasta dovodi do zagušenja zračnog prostora i preopterećenja pružatelja usluga u zračnom prostoru. Nove procedure i tehnologije uvode se svakodnevno, ali uz vrlo kritična testiranja. Simulacije su dio tih testiranja, no svaka simulacija je dobra koliko i model koji koristi. Tijekom studentskoga stažiranja u Eurocontrol-u, trenutni Base of Aircraft Data Family 4 (BADA 4) model je analiziran i istraženi su mogući segmenti poboljšanja klipno elisnih zrakoplova. Model klipno elisnih zrakoplova nije dobar koliko bi mogao biti, a u trenutnoj situaciji ga je potrebno poboljšati jer se povećava i broj zrakoplova generalne avijacije (uglavnom klipno elisni zrakoplovi). Tijekom istraživanja i analize trenutnog modela određeno je da je potrebno poboljšati model motora i model iskoristivosti elise. Podaci o krstarenju korišteni su kao primarni izvor podataka potrebnih za određivanje koeficijenta otpora zrakoplova u letu, također je dodana pretvorba vertikalne brzine u brzinu penjanja. Sa svim ovim poboljšanjima dobiveni su točni podaci o performansama u penjanju i krstarenju koji odgovaraju onim iz priručnika zrakoplova. Kao dodatan alat odrađena su dva ispitivanja u letu na različitim zrakoplovima. Rezultati testiranja u letu potvrdili su ispravno korištenje metoda za obradu podataka nakon testiranja koje koriste i proizvođači zrakoplova. Zaključno, sva određena poboljšanja predložena su Eurocontrol-ovom timu koji radi na BADA projektu, te njihova implementacija u BADA alat bit će odrađena ako se ustanovi da su predložena poboljšanja dobra i pridonose poboljšanju njihova modela.

Ključne riječi

Eurocontrol, Base of Aircraft Data (BADA), BADA Family 4 (BADA 4), simulacija, model, zračni promet, zračni proktor, klipni motor, elisa, performance, ispitivanja u letu, metode obrade podataka nakon ispitivanja u letu

Table of Contents

1.	Introduction.....	1
1.1.	Eurocontrol	2
1.1.1.	Directorate European Civil – Military Aviation (DECMA)	3
1.1.2.	Simulations and validation	3
1.2.	Base of Aircraft Data (BADA)	4
2.	BADA 4 modelling process	6
2.1.	Atmosphere model.....	6
2.1.1.	Atmospheric definitions.....	6
2.1.2.	Atmospheric expressions	7
2.2.	Aircraft model	12
2.2.1.	Current BADA 4 piston propeller model.....	13
2.2.2.	Gravitational group	13
2.2.3.	Aerodynamic group	14
2.2.4.	Propulsive group.....	16
3.	Research and development	18
3.1.	Engine power model.....	26
3.1.1.	Normally aspirated engine power model.....	27
3.1.2.	Pre-charged engine power model.....	32
3.2.	Propeller efficiency model	36
3.2.1.	Fixed pitch propeller efficiency.....	37
3.2.2.	Variable pitch propeller efficiency	41
3.3.	Drag polar	43
3.4.	Vertical speed / Rate of Climb conversion.....	49
4.	Analysis of the improved model segments.....	51

4.1.	Engine performance model.....	51
4.2.	Propeller efficiency model	53
4.3.	Drag polar	53
4.4.	Vertical speed / Rate of climb conversion	55
4.5.	Summary of the improved segments.....	58
5.	Flight tests	61
5.1.	Flight test segments.....	61
5.2.	Flight test conduction	62
5.3.	Flight test data reduction methods.....	64
5.3.1.	PIW – VIW data reduction method	64
5.3.2.	PIW – CIW data reduction method	65
5.3.3.	PIW – NIW.....	66
5.4.	Cessna Flight Test	66
5.5.	Diamond Flight Test.....	70
6.	Discussion.....	73
7.	Conclusion	77
	Bibliography	78
	List of Figures	79
	List of Tables	81
	List of Equations	82
	List of Labels.....	85
	Appendix A.....	87

1. Introduction

With the increase in air traffic, due to the air travel demand, air navigation service providers are overwhelmed with air traffic as the sky over Europe becomes overpopulated. To suppress this, air navigation service providers keep researching and developing, in cooperation with other participants in aeronautical research, new internal and public operational procedures. Simulations are one of the tools used in both research, development and implementation, but each simulation is as good as the model it uses. To this point the model used in the simulations was sufficient, but with these increasing trends the simulations need to be more precise and concise. Current BADA models don't include precise models of piston powered aircraft due to the fact that the percentage of them in reference to the other air traffic is minimal. Most of the traffic today consists of commercial jet transport aircraft, but with the increase in the overall numbers, the general aviation aircraft (mostly piston powered aircraft) start to introduce new challenges as they aren't often considered within the air traffic simulations. For that reason, it is necessary to improve the current piston propeller model.

All round better performing piston propeller model, which would replace the current models, will result in better understanding of general aviation traffic and its needs both for airspace and air navigation services. New model would enable more precise simulations, which would result in better insight for future development for coping with this increasing trend in air traffic. New methods and operational procedures could be established with regard to an improved model, enabling less congestion in air and on the ground.

As a general information chapter 1 provides some background data on both the Eurocontrol and Base of Aircraft Data (BADA).

Base of Aircraft Data Family 4, is the currently developed database and the introduction to the modelling process is described in chapter 2. BADA 4 piston propeller model is also addressed in the same chapter.

Chapter 3 contains analysis of the initial BADA 4 piston propeller model as well as all the research and development of the proposed improvements to the model.

Separate improvements are analysed and their individual contribution is described in chapter 4.

Final analysis and conclusion are located in chapter 7.

1.1. Eurocontrol

Aviation is the most growing mode of transportation in today's world. This vast network of big airports, invisible lanes and diverse set of aircraft doesn't need only to be maintained in current condition, but the future growth needs to be accommodated in advance.

One of these supporting organizations in Eurocontrol, European Organization for the Safety of Air Navigation [1]. This international organization was founded in 1963, with a working goal to achieve safe and seamless air traffic management across Europe [2]. Eurocontrol has 41 European member states, and two states in agreement outside Europe [1].

Eurocontrol is situated in four locations, its headquarters are in Brussels, Belgium. Most of the research and development activities take place in their Eurocontrol Experimental Center in Brétigny-sur-Orge, France. Institute of Air Navigation Training (IANS) is in Luxembourg, while the Maastricht Upper Area Control Centre (MUAC) is located in Maastricht, Netherlands.

The organization employs around two thousand people, and operates with an annual budget in excess of half a billion Euro [2].

Lot of effort in Eurocontrol is oriented towards students as they have a very strong traineeship program. Every student has an opportunity to apply for the traineeship, and if accepted a lot of support and help is offered to each one. For research, thesis or other kind of traineeship every student can choose in which way he wants to be involved and on which field of study he wants to participate.

1.1.1. Directorate European Civil – Military Aviation (DECMA)

Directorate European Civil – Military Aviation (DECMA) is one of the subdivisions of Eurocontrol, and its activities are more focused towards the research, development and implementation of the new technologies and procedures.

DECMA is a result of the merger of two former directorates, and it is an origin of innovation in all aviation domains, focusing on the fields with the biggest impact factor.

With the numerous past projects and new research, the European sky limits are pushed further every day.

1.1.2. Simulations and validation

Simulations are a major tool of the Eurocontrol organization, as they provide the necessary insight in future development and contribute in future major decisions.

All the new solutions brought to the aviation industry is thoroughly tested, for this instance simulations are one of the best solutions. Validation of various solutions is necessary, as the impact of these solutions can be quite marginal in some situations.

Simulations offered by Eurocontrol can be done in any part of the air traffic situation and phase, from airport, to airspace and control simulations.

As these simulations are air traffic oriented, the major complication that occurs is a sole number of aircraft types operating inside the simulated airspace. Every aircraft manufacturer bring something new to the market with every aircraft type it produces. These aircraft vary in size, capacity, speed, range, operating ceiling and other operational limitations and factor. All of these factors and limitations need to be modelled precisely for both the model performance and realism.

As the aircraft get more advanced, and the simulation technology becomes more powerful, the simulation precision and realism need to follow this trend. But every simulation is as good as the model that it uses.

Model and aircraft data used in Eurocontrol simulations is contained in a database called Base of Aircraft Data (BADA).

1.2. Base of Aircraft Data (BADA)

Base of Aircraft Data (BADA) is a database that contains both the model and aircraft specific coefficients and variables.

With the combination of the two, it is possible to reproduce aircraft performance throughout all flight phases. It enables realistic reproduction of geometric, kinematic and kinetic aspects of aircraft's behaviour.

Family 3 of BADA is the previous version of the database and models almost all aircraft types operating within ECAC area, but with certain error in the results of simulation.

To improve the precision of the model the databases are updated until they become officially released and locked to the final version. For further improvement it is required to use the newer release of BADA, currently BADA Family 4.

Newer release of BADA contains new models with new required coefficients for each aircraft type, but it doesn't contain all the types. By further updates this will change until final release of the Family 4.

BADA is used internationally as a reference in aircraft performance modelling for trajectory prediction and simulation. Mainly the BADA users are large communities such as research institutions, universities, air navigation service providers and many others.

With the new BADA Family 4, the performance and precision is increased over the entire flight envelope of the aircraft, which enables modelling and simulation of advanced systems and new concepts.

BADA model is based on mass varying, kinetic approach. Modelling an aircraft as a single point containing all the mass upon which the forces are acting.

Alongside the Aircraft Performance Model (APM) which is one group of components for the aircraft type, the Airline Procedure Model (ARPM) is used as a guideline to the exploit of the performance model. Through different flight phases it is possible to exploit the aircraft in different way, for that reason the airline procedure model determines the correct way of balancing the aircraft performance [1].

As the BADA 3 is already developed and locked to the current release, the future improvements in this paper are developed for the BADA 4.

All the future improvements are only a suggestion developed in collaboration with Eurocontrol, and as the owner of BADA concept the Eurocontrol needs to determine if the research is providing any improvement to their piston propeller model, and if the possible improvements are to be implemented.

2. BADA 4 modelling process

Base of Aircraft Data Family 4 (BADA 4) is a combination of two separate components, each representing an important structure in aviation modelling. One of them is an atmosphere model, which as a result generates all the required atmosphere properties. The second component, the main one, is an aircraft model, which should accurately represent aircraft actions, motion, operations, limitations, and performance [3].

2.1. Atmosphere model

An atmosphere is a layer of gases surrounding a planet, held in place by the gravity of the planet. The Earth atmosphere is mixture of nitrogen ($\approx 78\%$), oxygen ($\approx 21\%$), argon ($\approx 0,9\%$), carbon dioxide ($\approx 0,04\%$) and other gases in small amounts. Atmospheres content determines its major properties and these can be represented by a set of equations. Some of these equations are listed in chapters to follow, as they're important for some of future calculations, and may be used as references.

2.1.1. Atmospheric definitions

Geopotential altitude H [m] is that which under the standard constant gravitational field provides the same differential work performed by the standard acceleration of free fall when displacing the unit of mass a distance dH [m] along the line of force, as that performed by the geopotential acceleration when displacing the unit of mass a geodetic distance dh [m] [3].

Geopotential pressure altitude H_p [m] is the geopotential altitude H [m] that occurs in the ISA atmospheric conditions [3].

International standard atmosphere (ISA) is a static atmosphere model of how the pressure, temperature, density and viscosity of the Earth's atmosphere change with the change in altitude [4].

Mean sea level standard atmosphere conditions are those that occur in the ISA at the point where the geopotential altitude is zero. These values are stated below [3]:

Equation 1: Standard atmospheric temperature at MSL

$$T_0 = 288.15 \text{ K}$$

Equation 2: Standard atmospheric pressure at MSL

$$p_0 = 101325 \text{ Pa}$$

Equation 3: Standard atmospheric density at MSL

$$\rho_0 = 1,225 \text{ kg/m}^3$$

Equation 4: Standard speed of sound at MSL

$$a_0 = 340,294 \text{ m/s}$$

Tropopause is the boundary in the Earth's atmosphere, it stands above troposphere and below stratosphere. It is a boundary at which the temperature gradient changes, and its altitude depends on the latitude [3].

Equation 5: Average tropopause altitude

$$H_{p_{trop}} = 11000 \text{ m}$$

2.1.2. Atmospheric expressions

In reality standard atmospheric conditions rarely occur, for that reason there are equations that can describe the required atmospheric values. As the equations are based on physics, some required physical constants are provided below.

Equation 6: Adiabatic index of air

$$\kappa = 1,4$$

Equation 7: Specific gas constant for air

$$R = 287,05287 \text{ J/kg K}$$

Equation 8: Gravitational acceleration

$$g_0 = 9,80665 \text{ m/s}^2$$

Equation 9: ISA temperature gradient below tropopause

$$\beta_T = -0,0065 \text{ K/m}$$

Temperature can be determined easily with use of altitude and temperature gradient [3].

Temperature change with altitude can be seen on Figure 1.

Equation 10: Temperature for altitudes below tropopause

$$T = T_0 + \beta_T \cdot H_p \text{ [K]}$$

Equation 11: Temperature for altitudes at and above tropopause

$$T = T_{trop} \text{ [K]}$$

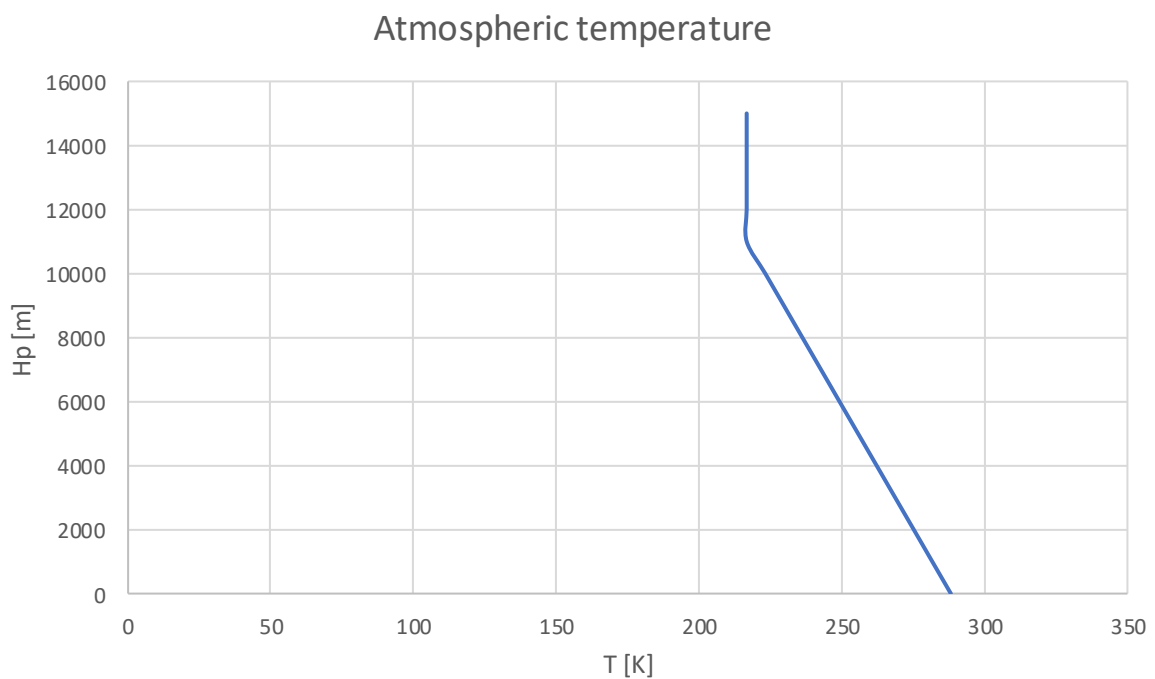


Figure 1: Atmospheric temperature up to 15000 m

Pressure is calculated by using the following equation [3]. Pressure change with altitude can be seen on Figure 2.

Equation 12: Air pressure for altitudes below tropopause

$$p = p_0 \left(\frac{T_{ISA}}{T_0} \right)^{\frac{g_0}{\beta_T \cdot R}} \text{ [Pa]}$$

Equation 13: Air pressure for altitudes at and above tropopause

$$p = p_{trop} \frac{g_0}{R \cdot T_{ISA_{trop}}} (H_p - H_{p_{trop}}) \text{ [Pa]}$$

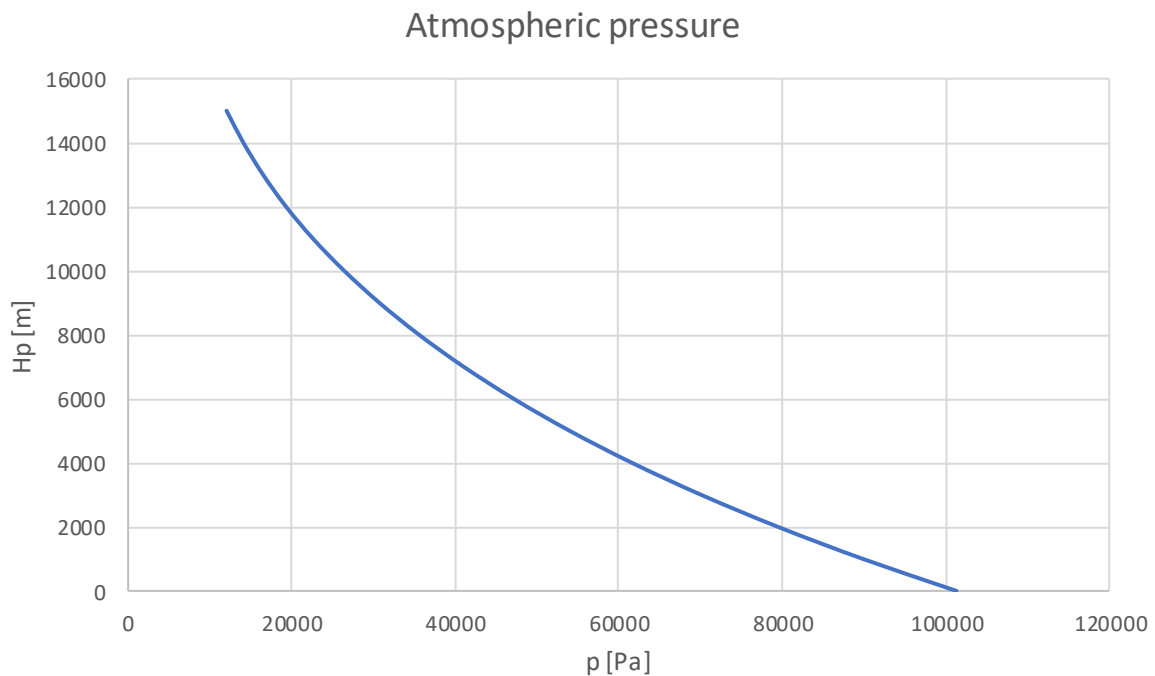


Figure 2: Atmospheric pressure up to 15000 m

Determination of air density is through the perfect gas law by using the already known temperature and pressure at a given altitude [3]. Density change with altitude can be seen on Figure 3.

Equation 14: Air density according to perfect gas law

$$\rho = \frac{p}{R \cdot T} \text{ [kg/m}^3\text{]}$$

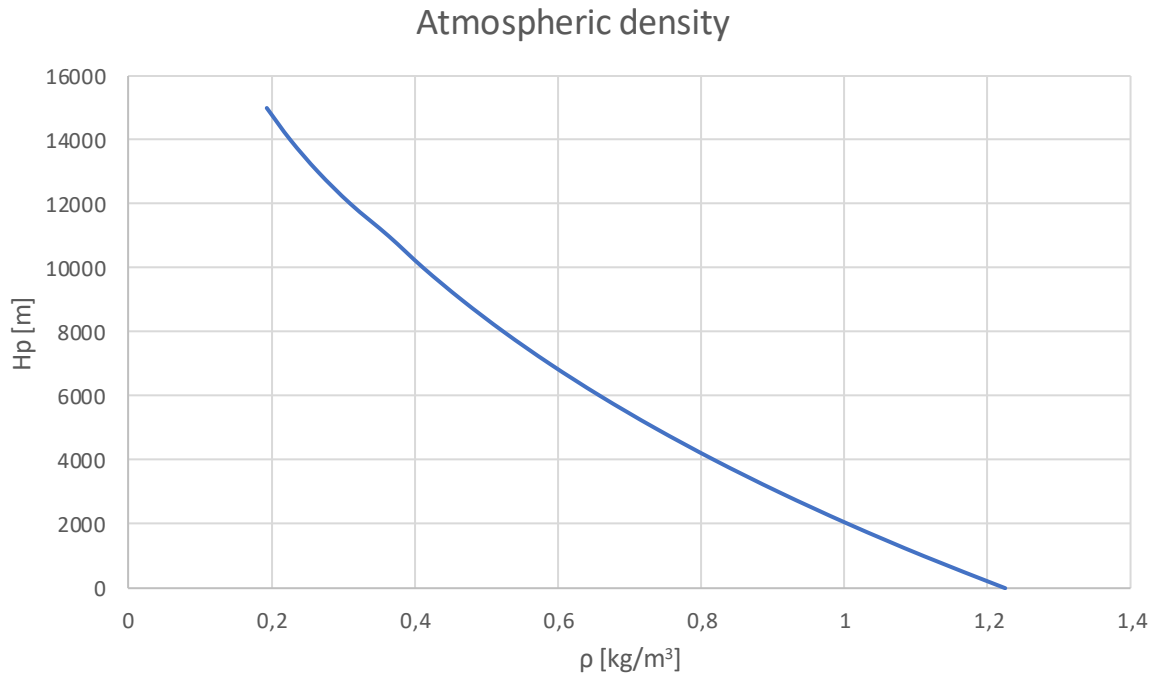


Figure 3: Atmospheric density up to 15000 m

All air characteristics can be represented as dimensionless values with standard values as references. The equations are as follows [3].

Equation 15: Temperature ratio

$$\theta = \frac{T}{T_0}$$

Equation 16: Pressure ratio

$$\delta = \frac{p}{p_0}$$

Equation 17: Density ratio

$$\sigma = \frac{\rho}{\rho_0}$$

The speed of sound is a speed at which the pressure waves are travelling through the fluid in which the temperature is as used in the equation below [3].

Equation 18: Speed of sound

$$a = \sqrt{\kappa \cdot R \cdot T} \text{ [m/s]}$$

Measuring speed in an aircraft is conducted by usage of pitot static systems, this speed is called indicated airspeed (IAS). It is used for aircraft operation, but this speed isn't useful for flight planning or aerodynamic calculations. For that purpose, the speed needs to be converted to true airspeed (TAS). This is possible by using the conversion equation, but this equation requires the input of calibrated airspeed (CAS) which is indicated airspeed corrected for instrument errors and position error. Calibrated airspeed is usually obtained by referring to aircraft manual with known indicated airspeed. The equations for converting the calibrated airspeed to true airspeed and true airspeed to calibrated airspeed are given below [3].

Equation 19: Calibrated to True airspeed conversion

$$v_{TAS} = \left(\frac{2 \cdot \kappa \cdot p}{\kappa - 1 \rho} \left[\left\{ 1 + \frac{p_0}{p} \left(\left[1 + \frac{\kappa - 1 \rho_0}{2 \cdot \kappa \cdot p_0} v_{CAS}^2 \right]^{\frac{\kappa}{\kappa - 1}} - 1 \right) \right\}^{\frac{\kappa - 1}{\kappa}} - 1 \right] \right)^{\frac{1}{2}} \text{ [m/s]}$$

Equation 20: True to Calibrated airspeed conversion

$$v_{CAS} = \left(\frac{2 \cdot \kappa \cdot p_0}{\kappa - 1 \rho_0} \left[\left\{ 1 + \frac{p}{p_0} \left(\left[1 + \frac{\kappa - 1 \rho}{2 \cdot \kappa \cdot p} v_{TAS}^2 \right]^{\frac{\kappa}{\kappa - 1}} - 1 \right) \right\}^{\frac{\kappa - 1}{\kappa}} - 1 \right] \right)^{\frac{1}{2}} \text{ [m/s]}$$

The aircraft speed can also be given as a dimensionless quantity represented by speed of sound [3].

Equation 21: Mach number

$$M = \frac{v_{TAS}}{a}$$

Equation 22: True airspeed from Mach number

$$v_{TAS} = M \cdot a \text{ [m/s]}$$

For the determination of aerodynamic forces it is also required to know the dynamic pressure, this can be easily calculated by using the following expression.

$$q = \frac{1}{2} \cdot \delta \cdot p_0 \cdot \kappa \cdot M^2 \text{ [Pa]}$$

2.2. Aircraft model

BADA aircraft model is based on mass-varying, kinetic approach to modelling. Model itself is structured into three major parts: the Aircraft Performance Model (APM), the Airline Procedure Model (ARPM) and the Aircraft Characteristics.

Aircraft Performance Model represents aircraft's actions, forces that act upon the aircraft in flight and result in its motion. This category is subdivided into gravitational, aerodynamic and propulsive group of forces. Alongside the aircraft's actions, aircraft's motion consists of a certain equation set that model the aircraft motion. Operations model describes different ways or procedures for operating the aircraft, and limitations model determines, or limits, the aircraft behaviour to realistic flight.

Aircraft Procedure Model provides the model with all the required speeds and configurations during different flight phases throughout normal aircraft operations, such as:

- takeoff
- climb
- cruise
- descent
- approach
- landing

Aircraft Characteristics, which contains all the aircraft specific values or coefficients, such as drag polar coefficients, power, propeller efficiencies and similar. The entire model is based on a mass-varying, kinetic approach to aircraft performance modelling [3].

Most of the piston propeller powered aircraft in use today are general aviation aircraft with low maximum takeoff masses. This allows for very simple approach to the modelling process,

due to the fact that the configuration of these aircraft is very simple and limited. Their aerodynamic characteristics are simple and are influenced by changes in configuration in a simple way. This change can easily be described by simple addition or reduction of the already calculated coefficients. Same principle applies to the powertrain, there are a few possible combinations available, and all of them will be addressed separately.

Goal of the model is successful replication of the performance data available in the airplane's flight manual. Most valuable performance groups that need to be modelled accurately are climb and cruise performance groups. Both of them should be modelled in a way that the performance is a result of a few input points available from climb and cruise data already available in the airplane flight manual.

2.2.1. Current BADA 4 piston propeller model

Aircraft motion is a result of multiple forces acting on the aircraft itself. These forces can be divided into three major groups. First group of the three is gravitational, and it contains the gravitational force on the aircraft. Second group is the aerodynamic group which contains the aircraft's lift and drag forces. And last group of the three is the propulsive group which contains engine power, thrust and propeller efficiency [3].

An aircraft is a non-rigid object moving through space. For the simplicity of the calculation in most simulations, at least ones that are oriented towards performance of the aircraft, all aircraft are assumed to be rigid objects. This allows the model to be more concise and simpler. For all the following calculations the aircraft will be considered a rigid object, enabling for the forces to act upon aircraft centre of gravity.

2.2.2. Gravitational group

The gravitational force acting upon the aircraft, known as aircraft's weight, is a force that is assumed to be acting on an aircraft's centre of gravity pulling it towards Earth's centre of gravity. The intensity of this force can be calculated using the following expression .

Equation 24: Aircraft weight

$$F_G = m \cdot g_0 \text{ [N]}$$

2.2.3. Aerodynamic group

Aerodynamic forces are result of the interaction between bodies and airflow. These reactions are highly influenced by the state of the air flowing over them, shape and other properties of the bodies. Configuration changes also greatly affect the magnitudes of these forces and their corresponding coefficients.

Aerodynamic coefficients are dimensionless values which link aerodynamic forces with dynamic pressure and aircraft's reference surface, usually it's wings surface. When discussing the aerodynamic reactions of bodies travelling through air, it is more convenient to use coefficients as they are more representative values than the forces themselves. This is because the airplanes of different size posses different wings size and require different magnitude of force. An example of connection between the force and its coefficient is stated below.

Equation 25: Aerodynamic force

$$F = c \cdot q \cdot S_{ref} \text{ [N]}$$

Equation 26: Aerodynamic coefficient

$$c = \frac{F}{q \cdot S_{ref}}$$

Most of the aircraft posses some sort of devices that make changes to its exterior shape which influence the airflow and resulting forces. These devices always have both positive and negative influence on the aerodynamic coefficients. High lift devices, also known as flaps, are used to increase the lift of a surface at lower speeds, their negative effect is an increase in drag. On the other hand, sometimes it is wanted to increase the drag so that the airplane could slow down or lose a certain amount of altitude. These devices are called spoilers, they increase the drag, and lower the amount of lift generated by the wings. Some other types of devices that have an influence on aerodynamic coefficients are cowl flaps, retractable

undercarriage or wheel fairings on fixed undercarriages. That said it is always important to be aware of the aircraft's configuration.

To simplify some expressions, assumptions had to be made. All of these are stated for each of their corresponding coefficient and force.

The aerodynamic lift is a force acting perpendicular to the free airflow. The lift coefficient can be determined by the following expression. However, mind that the flight path angle is considered zero, because the airplanes typically cannot achieve big enough angle to introduce a significant error. The bank angle correction is required as the angles can be quite significant.

Equation 27: Aerodynamic lift coefficient

$$c_L = \frac{2 \cdot m \cdot g_0}{\delta \cdot p_0 \cdot \kappa \cdot S_{ref} \cdot M^2 \cdot \cos \varphi}$$

The aerodynamic drag of smaller airplanes can be modelled in a simple way, by using the expressions for the parasitic drag and induced drag. Parasitic drag is a part of the total drag, produced by form drag, or pressure drag, friction and interference drag. Induced drag is a product of additional airflow that is formed over the wing, this airflow is a result of pressure difference above and below wing surface. This pressure difference causes the air to flow around the wing tips from lower part to the upper part of the wing. After this vortex is formed, the downwash flow of air is formed behind the wings, this changes the effective direction of airflow over the wing tilting it downwards. By doing this the lift force is tilted backwards and a part of the lift is contributing to the drag force. Effect of induced drag, unlike the parasite drag, is smaller with increase of speed, also the higher wing aspect ratio contributes to the reduction of this drag component. The drag coefficient is a simple sum of the parasite and induced drag coefficients.

Equation 28: Aerodynamic drag coefficient

$$c_D = c_{D_0} + c_{D_i}$$

Determination of drag coefficients is very difficult without the full analysis of the entire aircraft, but there are certain methods that can be used for a good approximation.

2.2.4. Propulsive group

Airplanes can be powered by a single, or multiple engines of one available type. Single engines often provide a simpler environment for flight operation, but multiple engines provide a higher safety factor together with better performance.

Piston engines can be divided into certain groups by their design. They can be normally aspirated, where the engine intakes the air, or air and fuel mixture, by simply creating vacuum in its cylinders. The other major group of piston engines is the one where air is forced into engines cylinders. Further these engines can be divided by the method used to compress the air, one use the power of engine to compress the air by the means of supercharger, and other use the pressure of exhaust gasses to compress the air in the turbocharger. Power of these engines is modelled differently.

The power of an engine is modelled in the following way. This model is used to determine the power of an engine in standard conditions [3].

Equation 29: All engine power

$$\dot{W}_P = F_{Gref} \cdot a_0 \cdot c_P \text{ [W]}$$

The power coefficient is determined by usage of known data from the airplane's operating manual, and is a reference power coefficient for available power in standard atmosphere at mean sea level. The power coefficient is determined as follows [3].

Equation 30: Power coefficient

$$c_{P_{max,ISA;MSL}} = \frac{\dot{W}_{P1_{max,ISA;MSL}} \cdot n_{eng}}{F_{Gref} \cdot a_0}$$

This power coefficient is modified by throttle, this throttle parameter represents the throttle position in percentage [3].

Equation 31: Throttle regulated power coefficient

$$c_{P_{ISA;MSL}} = c_{P_{max,ISA;MSL}} \cdot \delta_T$$

Force induced engines are capable to maintain the maximum power until they reach the critical altitude. The critical altitude is an altitude above which the supercharger, or

turbocharger is unable to maintain the required pressure level. The power change of these engines is modelled as followed [3].

Equation 32: Power coefficient below critical altitude

$$C_P = C_{P_{ISA,MSL}}$$

Equation 33: Power coefficient above critical altitude

$$\min \left[C_{P_{ISA,MSL}}, C_{P_{max,ISA,MSL}} \frac{\delta}{\delta_{\rho_{turbo}}} \sqrt{\frac{\theta_{\rho_{turbo}}}{\theta}} \right]$$

The propeller efficiency is modelled through the propeller momentum theory as stated below.

Equation 34: Propeller efficiency

$$\eta = 2 \cdot \eta_{max} \left(1 + \left[1 + 2 \cdot \eta \frac{\dot{W}_P}{n_{eng}} \left\{ \sigma \cdot \rho_0 \cdot D_P^2 \frac{\pi}{4} v_{TAS}^3 \right\}^{-1} \right]^{\frac{1}{2}} \right)^{-1}$$

This expression can be written as a third degree polynomial equation, and finding the roots results in a propeller efficiency for a given conditions.

Equation 35: Propeller efficiency polynomial expression

$$2 \frac{\dot{W}_P}{n_{eng}} (\sigma \cdot \rho_0 \cdot D_P^2 \cdot \pi \cdot v_{TAS}^3 \cdot \eta_{max})^{-1} \cdot \eta^3 + \eta - \eta_{max} = 0$$

One of the ways to solve this expression and find the propeller efficiency is listed in Appendix A.

3. Research and development

Initial BADA 4 piston propeller model uses airplane's operating manual performance data as that data is provided by the manufacturer of the aircraft and can be trusted. Most of the required data is listed within performance part of the manual, while some odd pieces of information can be found elsewhere throughout the manual. Data obtained from other sources, such as radar tracks of the airplanes, is used only for comparison of the model with real traffic data.

For the performance part of the model, this includes drag, thrust, power and propeller efficiency, the reference data used is the climb data. In the airplane manual the reference values of rate of climb for different airplane conditions are presented in a graph or table. The main goal is to fit the correct drag, thrust, power coefficients to the model so that it replicates the data obtained from the manual.

The total energy model is used to obtain the required power of an airplane to climb at a specific speed and rate of climb.

Equation 36: Rate of climb / descent

$$ROCD = \frac{dH_p}{dt} = \frac{T_{ISA}}{T} \frac{(F_T - F_D)v_{TAS}}{m \cdot g_0} \left(1 + \left[\frac{v_{TAS}}{g_0} \right] \left[\frac{dv_{TAS}}{dh} \right] \right)^{-1} \text{ [m/s]}$$

As seen from the equation above the airplane's rate of climb or descent is a function of its drag, power and propeller efficiency.

For the initial values of these variables an iteration tool was used to obtain the best fit across the reference values.

From the start, as a test, a pair of data for each airplane was used. One of the data sets had all coefficients calculated as stated above, while the other had an additional efficiency factor, so-called efficiency correction. In combination with efficiency correction the drag coefficients were set arbitrarily. The main reason for this was incomprehension of the data available from the two different airplanes that share the same airframe but have different power plant options.

As an example of the existing initial state of the models, the obtained data presented in a form of power against altitude graph is shown in graphs below. Figure 4 and Figure 5 represent the required power for an aircraft with current coefficients to climb at a speed stated in the manual as best rate of climb speed with the rate of climb stated individually for each altitude. The available engine power is a result of the current engine power model. Figure 4 is generated with use of equations stated in chapters above, while Figure 5 is generated using the same set of equations with addition of previously mention efficiency correction. Both of these represent the data obtained in standard atmospheric conditions denoted as ISA. For non-standard conditions everything is calculated in the same manner with only difference of outside air temperature set to fixed values of negative twenty degrees Celsius as shown in Figure 6 and Figure 7. This is also repeated for the positive twenty degrees Celsius as presented in Figure 8 and Figure 9.

Analysis of these results indicate that the used coefficients and or models contain an unrecognized mistake. These will be addressed in the following chapters.

Climb Power - Altitude ISA (C182)

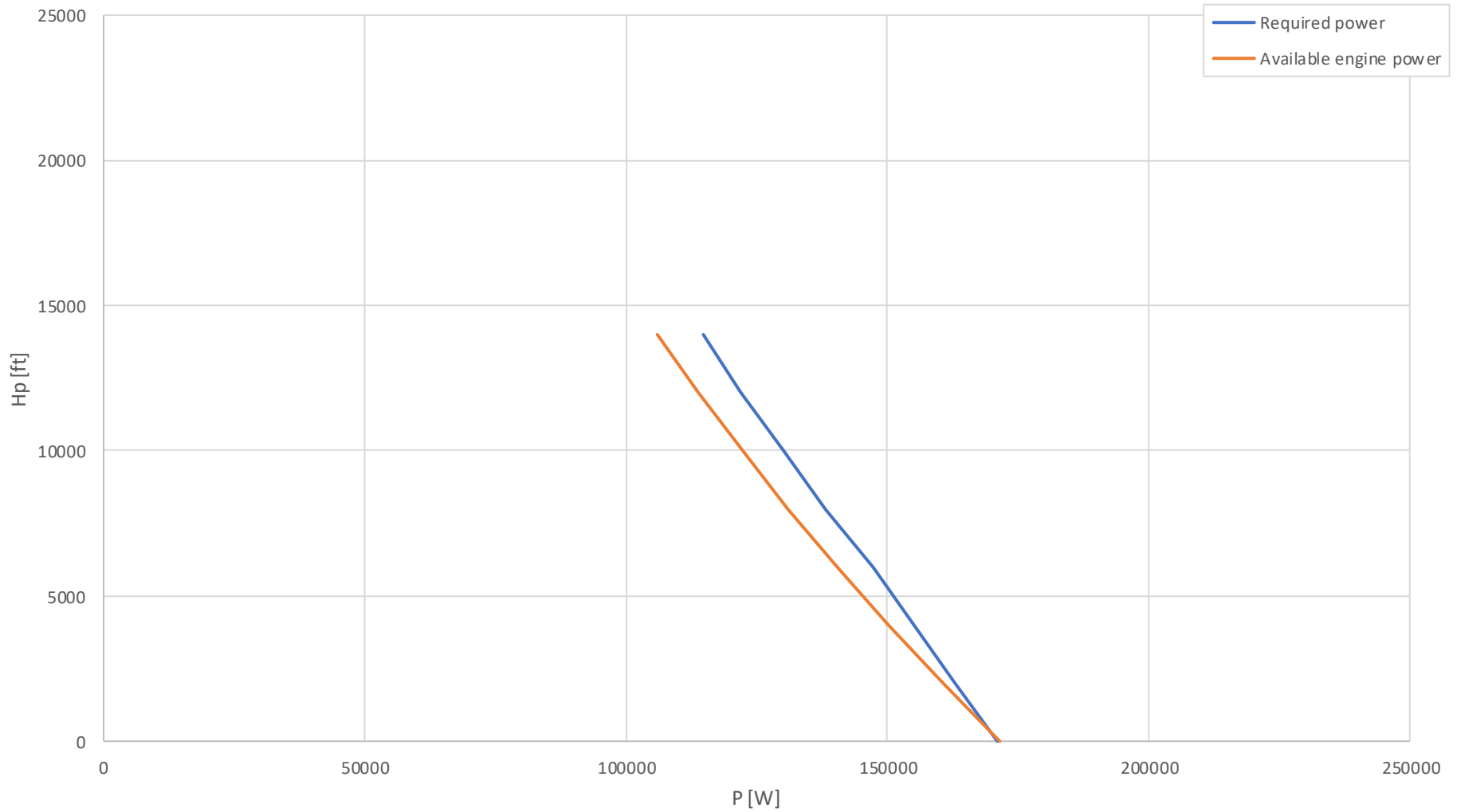


Figure 4: Climb Power - Altitude ISA graph for Cessna 182

Climb Power - Altitude ISA (C182) EC

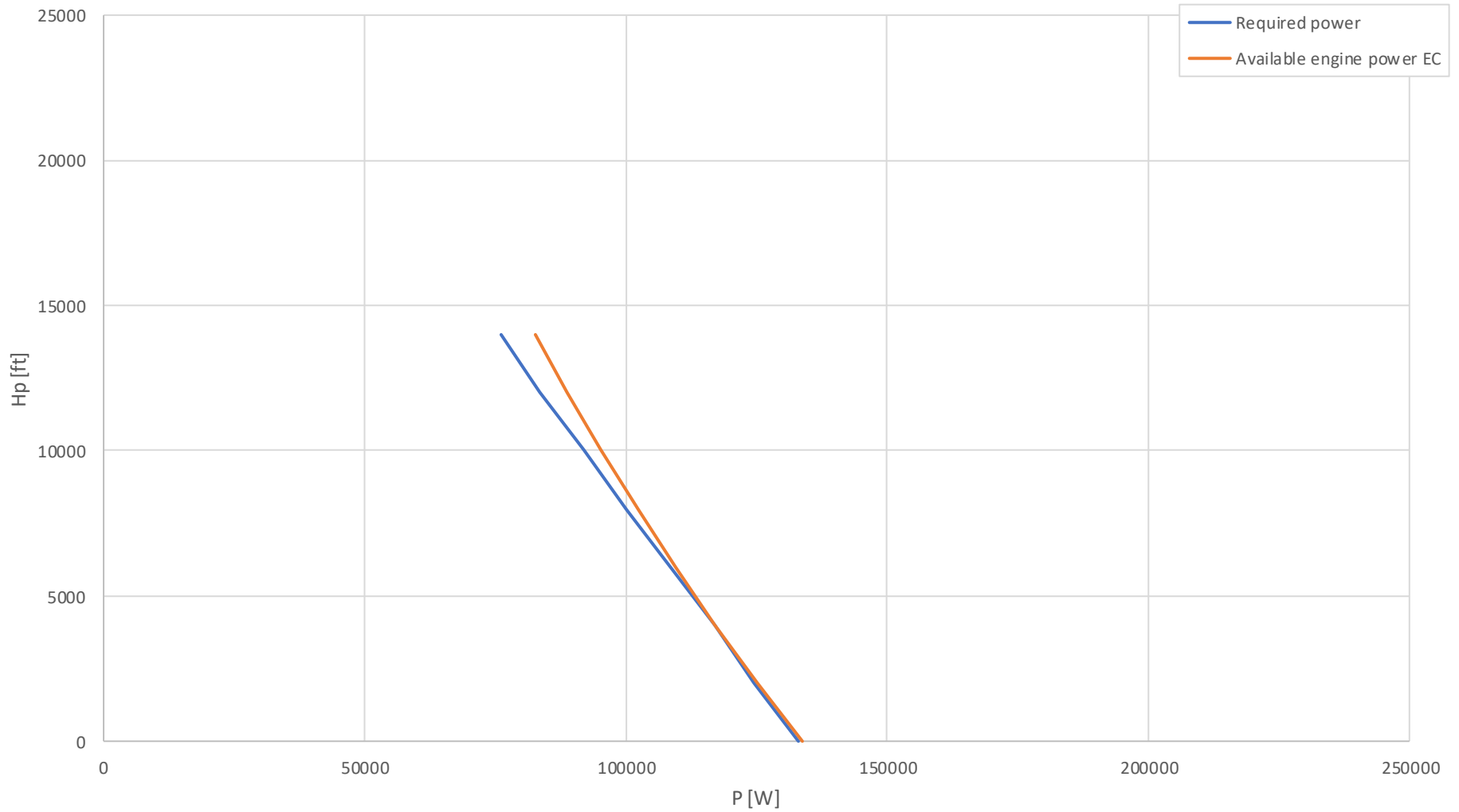


Figure 5: Climb Power - Altitude ISA graph for Cessna 182 with efficiency correction

Climb Power - Altitude OAT -20 °C (C182)

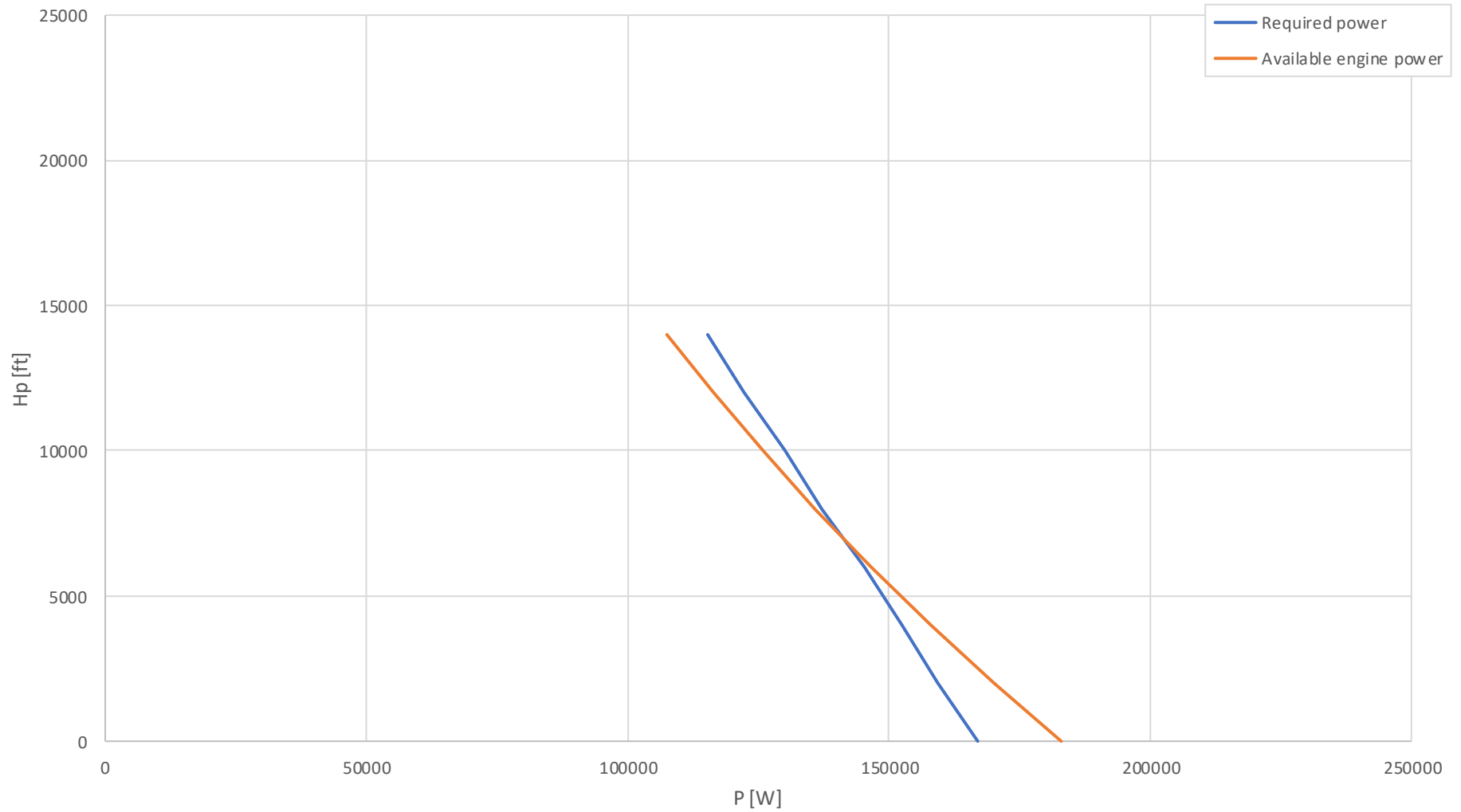


Figure 6: Climb Power - Altitude OAT -20 °C graph for Cessna 182

Climb Power - Altitude OAT -20 °C (C182) EC

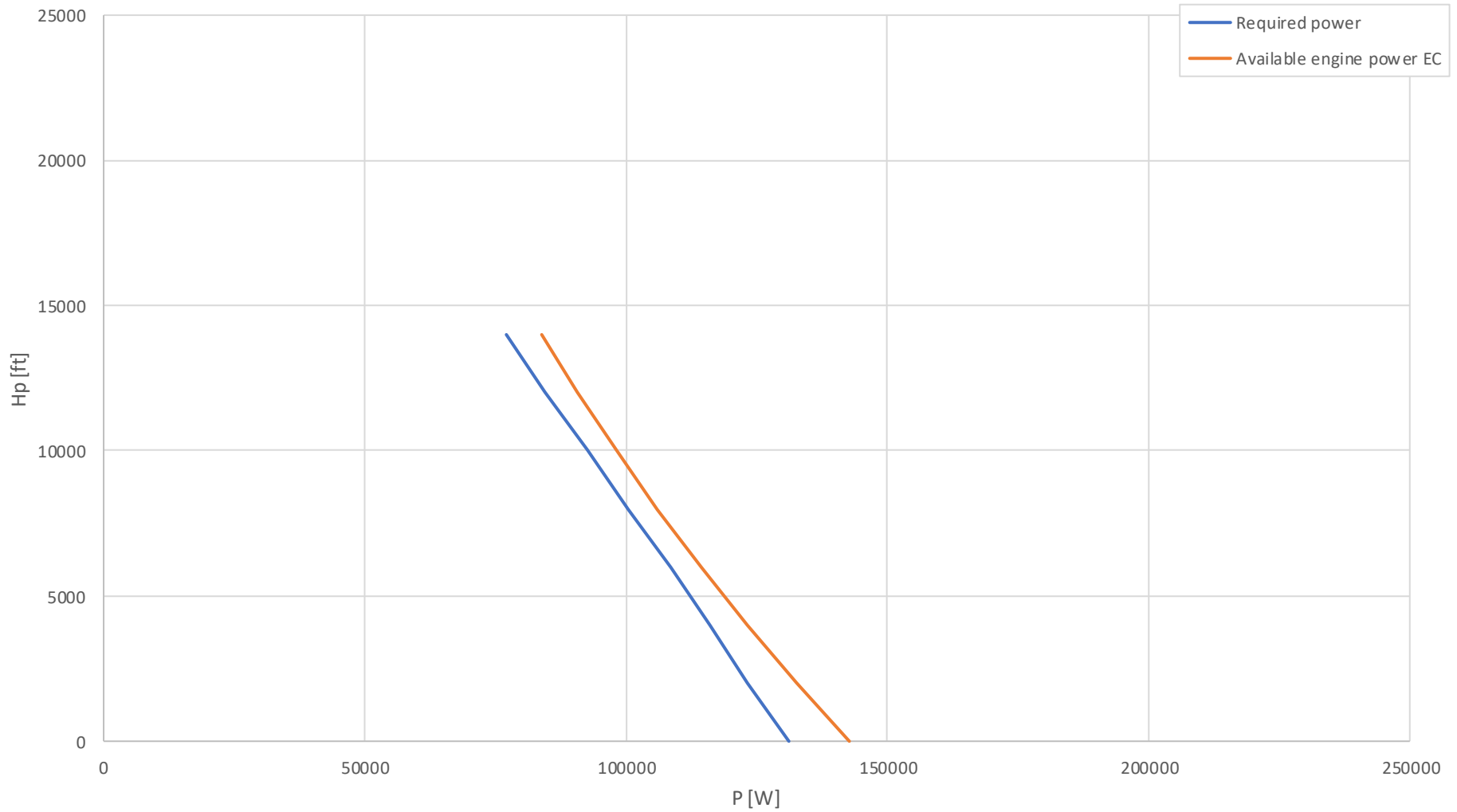


Figure 7: Climb Power - Altitude OAT -20 °C graph for Cessna 182 with efficiency correction

Climb Power - Altitude OAT +20 °C (C182)

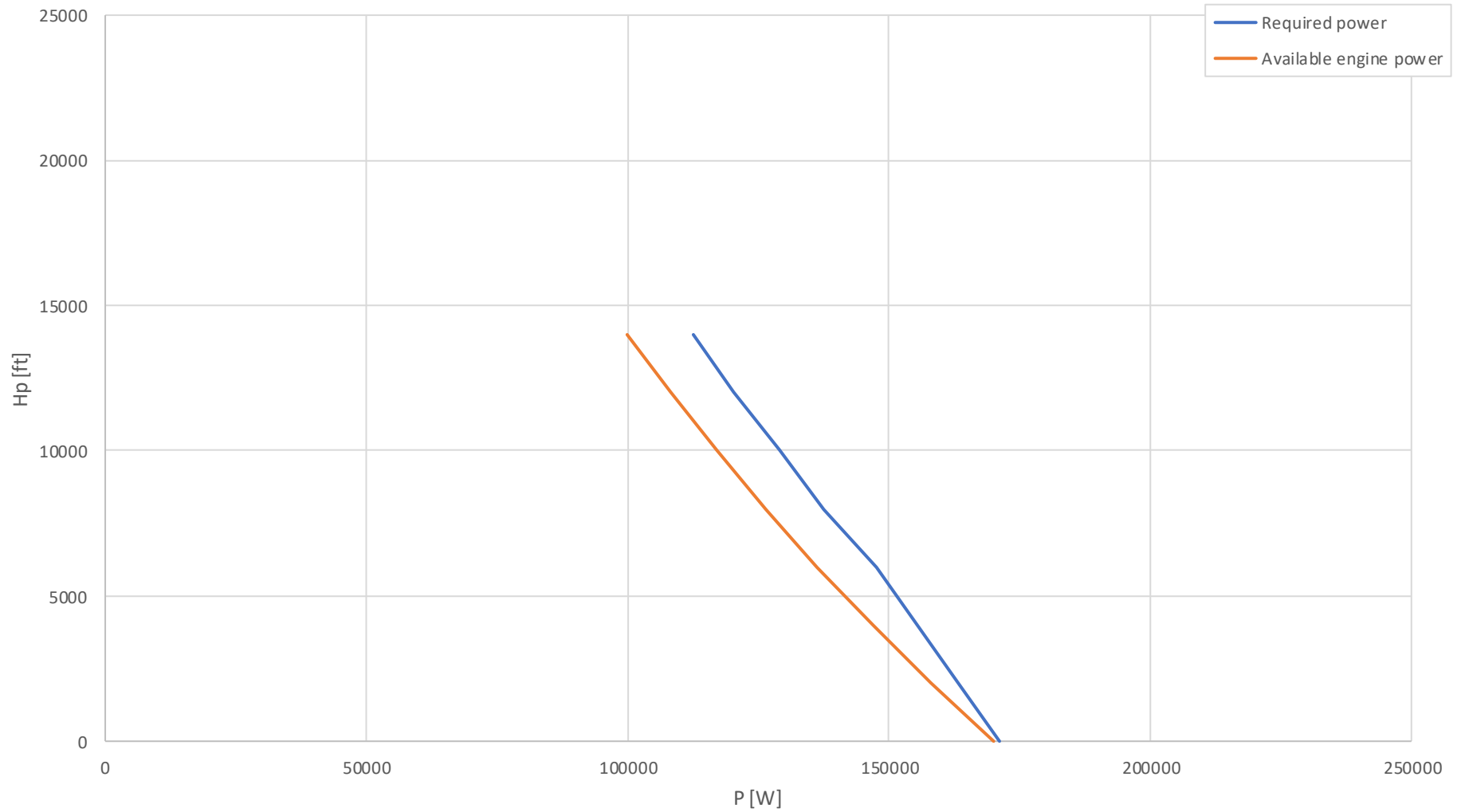


Figure 8: Climb Power - Altitude OAT +20 °C graph for Cessna 182

Climb Power - Altitude OAT +20 °C (C182) EC

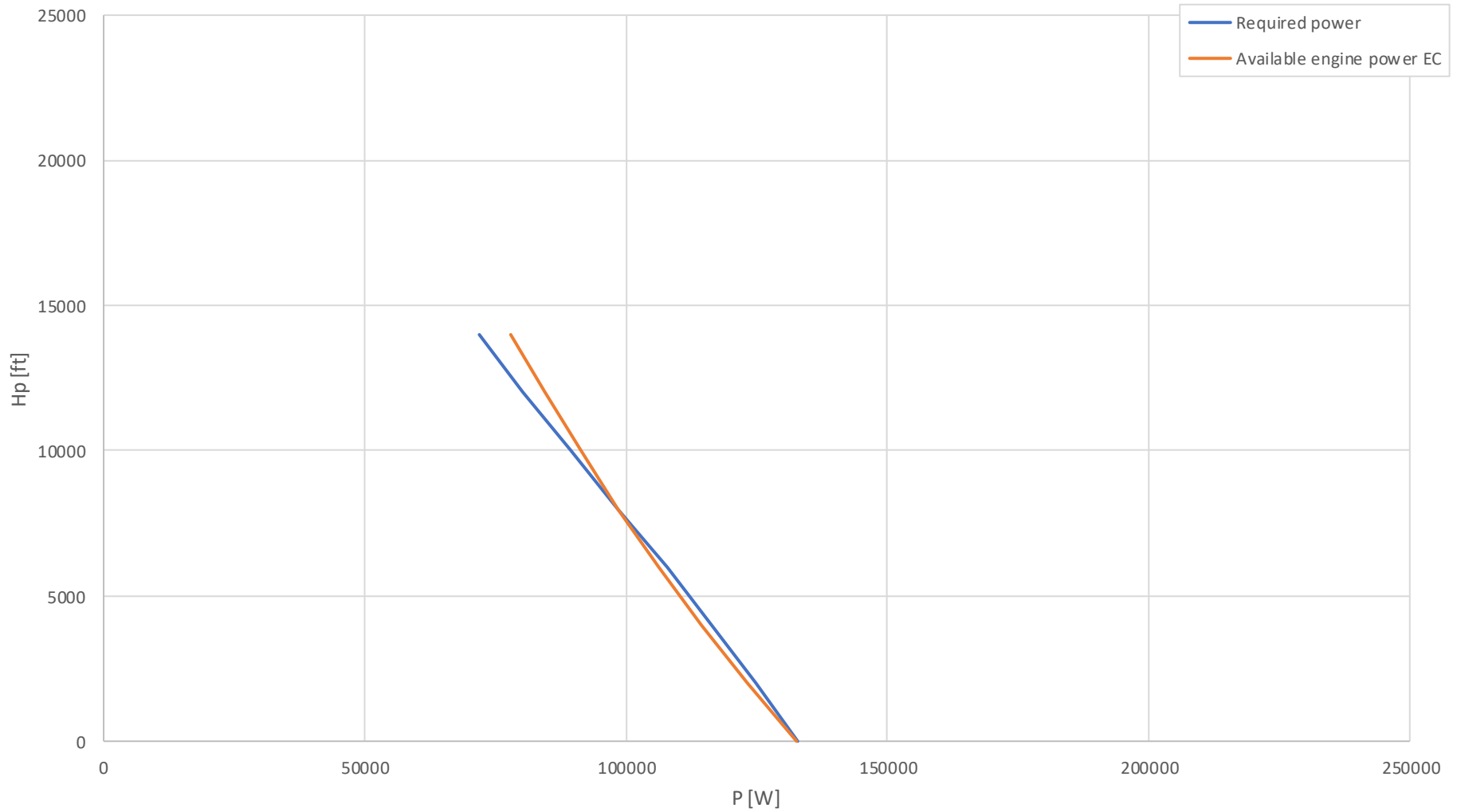


Figure 9: Climb Power - Altitude OAT +20 °C graph for Cessna 182 with efficiency correction

As continuation of work some existing coefficients or models are updated, or upgraded while some are exchanged with something new.

3.1. Engine power model

As stated earlier, most important part of model building is a sturdy reference. Engine power can be quite unpredictable and hard to model, but obtaining the correct and quite precise engine power model will greatly ease the following improvements to other aspects of this model.

Engine power model enables the maximum climb performance calculations. The maximum available power is obtained from the engine model, and this power is divided by the energy share factor between acceleration and climb.

Cruise performance is also limited by the engine power model, as the maximum power setting is obtained from the engine power model.

To model an engine power, as for every other model the reference data is very important. In pursuit for data few engine operator manuals were obtained and according to them the future models were developed.

Because we divided the piston engines into subcategories before, it is only appropriate to model the subcategories individually. The model for the normally aspirated engines will be examined first and after that the engines with forced induction.

Some problems encountered were differences between installed power and the engine power measured on the test bench. After some research, some sources indicate that difference between these two power values can go up to 10 %. This introduces an error in calculations from the start, but because this cannot be determined generally for all aircraft, and individual determination is impossible, a workaround is needed. Since the manufacturers don't provide this information, and state the same power value in their manuals as engine manufacturers in their manual do, then this is taken as reference. This should provide a good data source for the engine power model, since every engine is different and by assuming that the average offset of these engines wouldn't cause an issue. Other issue comes in form of

mixture leaning, with different mixture settings different maximum powers can be obtained. It is important to note that the following power models only represent power available if best power mixture is set.

3.1.1. Normally aspirated engine power model

Available power of the normally aspirated engines depends on how efficiently the engine can burn the air and fuel mixture inside its cylinders. The combustion of the mixture produces a sharp increase of pressure inside the cylinder, which as a result pushes the piston and transfers energy. The combustion highly depends on the amount of oxygen, fuel and their ratio. As the airplane climbs the surrounding pressure and density drop causing the decrease in oxygen available for the process of combustion. So, connection can be drawn between altitude and engine's performance [5].

Estimating the altitude impact on engine performance can be achieved using some models that rely on density ratio. The model which provides the best fit to the engine performance reference data is the Gagg and Ferrar model. The Gagg and Ferrar model is concise and simple, yet effective as the result provide a good fit between the model and reference data across multiple engine manufacturers. The model consists of an equation shown below.

Equation 37: Gagg and Ferrar engine performance model

$$P = P_{ISA,MSL} \frac{\sigma - 0,117}{0,883} \text{ [W]}$$

Unfortunately, this model only provides a good fit to the reference data in standard atmosphere conditions. For that reason, additional work was needed to improve the model and assure that it covers the non-standard atmospheric conditions. A resulting model contains the Gagg and Ferrar model calculated in standard atmospheric conditions corrected for the non-standard temperatures. This temperature should be used as carburettor air temperature (CAT), but in lack of available data, outside air temperature (OAT) is used as it is approximately the same as inlet temperature. While the OAT is good approximation for the temperature correction, the CAT is constantly offset from this value, it follows the OAT in change but the offset can be as big as ± 20 °C. It would be better if CAT was obtainable and if

it could be modelled simply, but this isn't the case. The final model uses OAT and is shown below.

Equation 38: Normally aspirated engine performance model

$$P = P_{ISA,MSL} \frac{\sigma_{ISA} - 0,117}{0,883} \sqrt{\frac{T_{ISA}}{T}} \text{ [W]}$$

Results of this model can be observed on the following graphs. Engine reference power represents the engine reference power obtained from the engine operating manual, while the engine model power represents the model output. Model was tested in standard atmospheric conditions denoted ISA, and non-standard conditions at outside air temperature set to fixed values of + 20 °C and – 20 °C. Figure 10 shows the reference data and model results for the Continental O-240-D engine which can be found on Cessna 162 airplane. The Lycoming IO-540-AB1A5 engine can be found on Cessna 182 airplane while its reference data and model results are presented in Figure 11. And Figure 12 contains the Rotax 912-S reference data with the model results, this engine can be found on Diamond DV20 airplane. Small deviations between reference data and model results can be explained as data reading mistake, because all the reference data was obtained by manually reading the data. The non-standard conditions were included as a reference as well, they were obtained by reading the values from the provided engine manuals and corrected by the appropriate correction stated in the vicinity of the diagrams in the manual (usually expressed as equation).

Power - Altitude Continental O-240-D (C162)

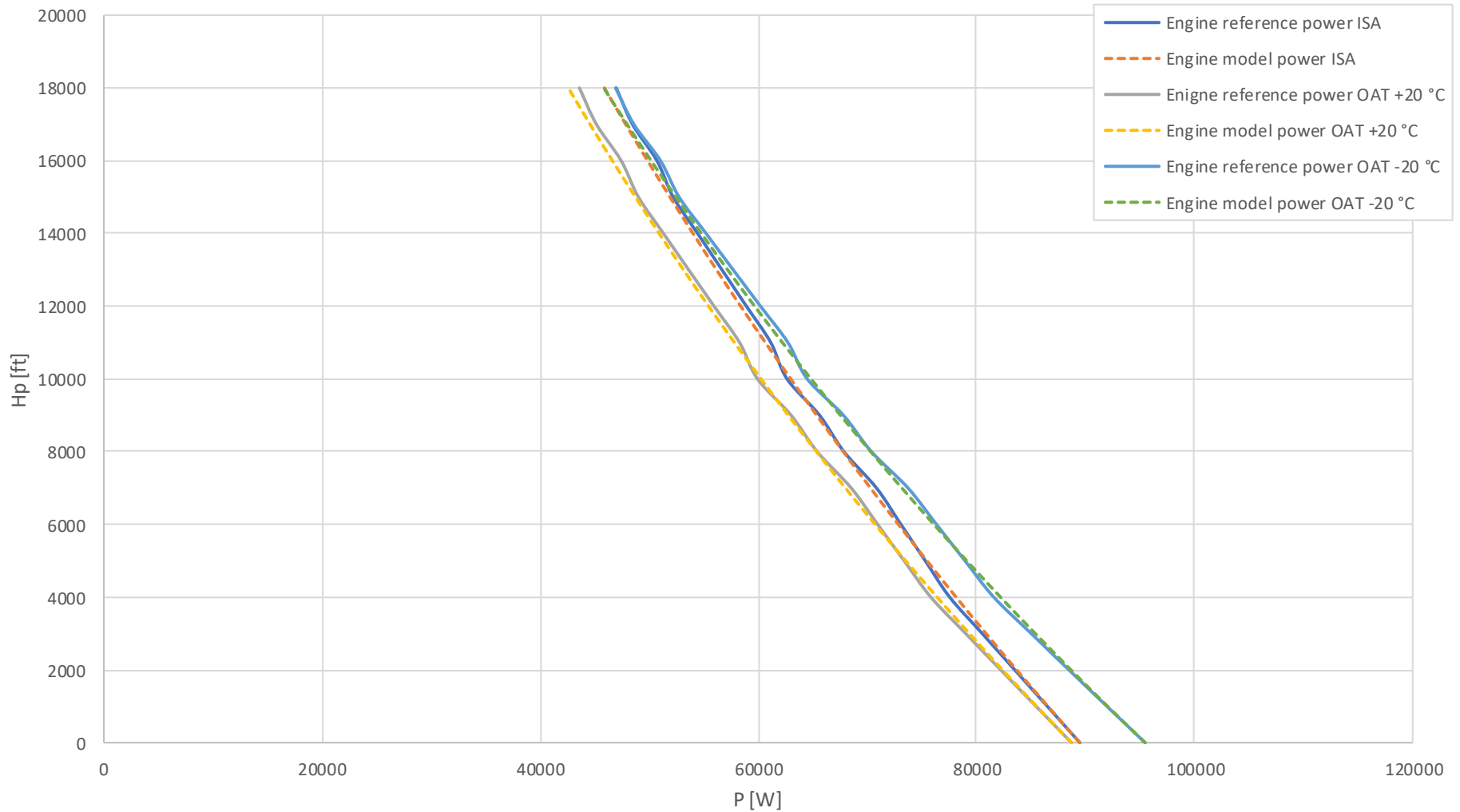


Figure 10: Power - Altitude graph for Continental O-240-D (C162)

Power - Altitude Lycoming IO-540-AB1A5 (C182)

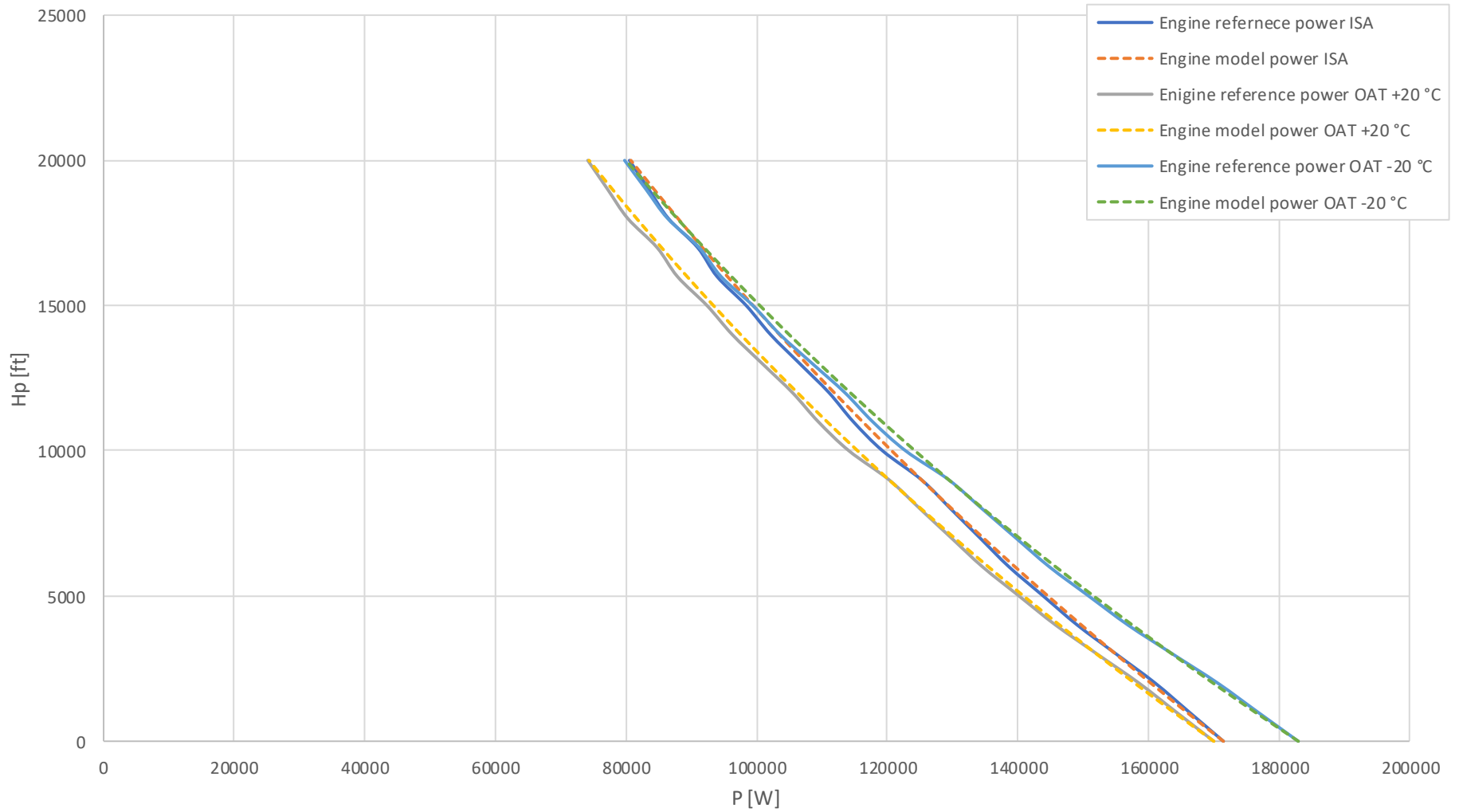


Figure 11: Power - Altitude graph for Lycoming IO-540-AB1A5 (C182)

Power - Altitude Rotax 912-S (DV20)

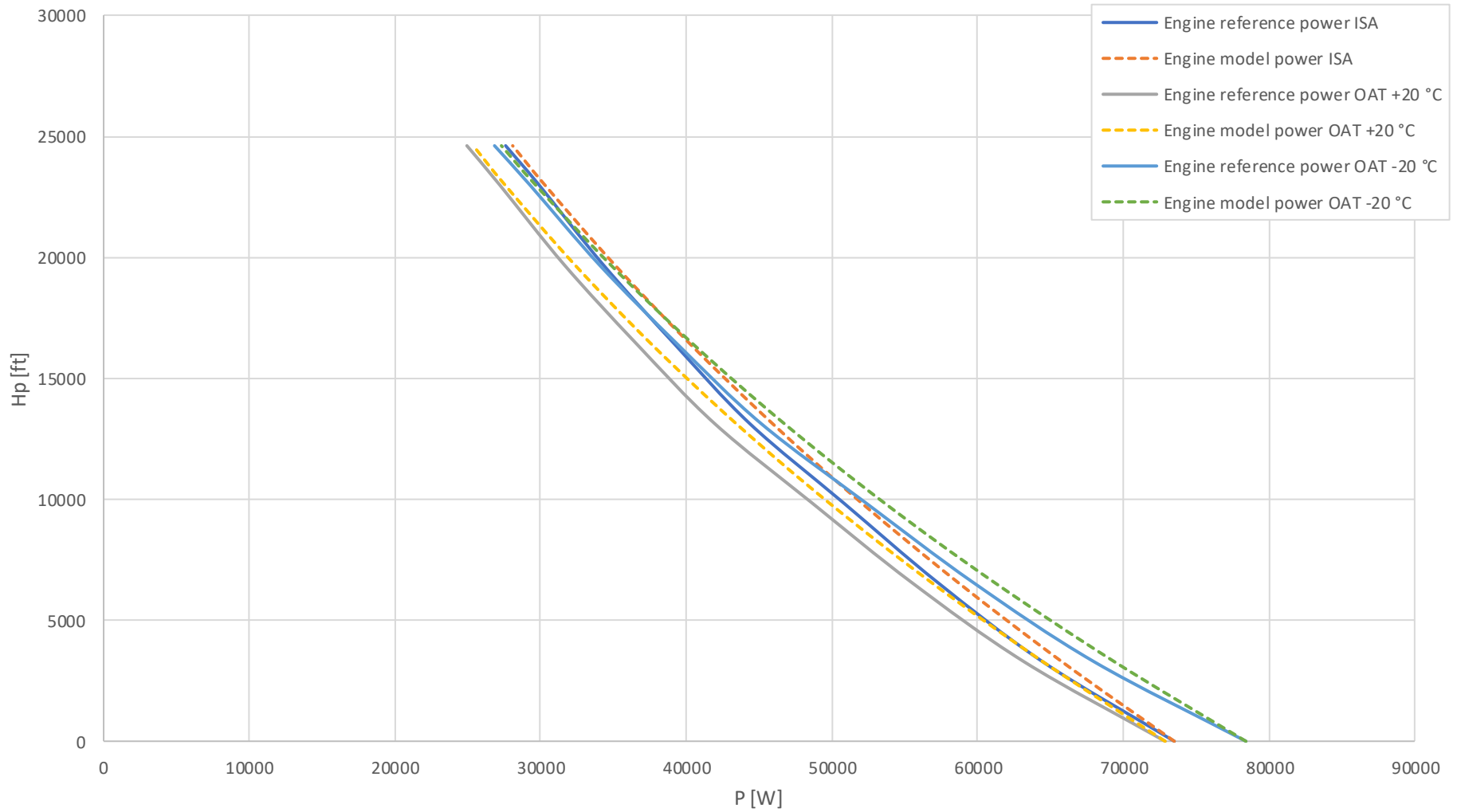


Figure 12: Power - Altitude graph for Rotax 912-S (DV20)

3.1.2. Pre-charged engine power model

Pre-charged engines, or force induction engines, are equipped with the additional device that enables them to compress the intake air to maintain the certain pressure. This compression enables them to maintain approximately same power up to the critical altitude, after which the surrounding air pressure is lower than required by the compressor to maintain constant intake pressure.

Engines can be equipped with the supercharger, which uses some engine power to compress the air to the required level. Or, they can be equipped with the turbocharger, which uses the pressure of the exhaust gases to power the compressor. Turbocharged engines are often more efficient than the supercharged. They use exhaust gas flow over the turbine as the intake power for the compressor, while the superchargers are directly attached to the engine and take power directly from the engine. Turbocharged systems are a fail-safe as they can be disengaged in case of failure, while the supercharger continuous to spin due to the direct connection to the engine.

Unrelated to the type of the charging system, the systems can be set to affect the intake pressure in two ways. One of them is to maintain the intake pressure at a maximum of standard pressure at mean sea level, and the other is to raise and maintain the pressure at a maximum which is above standard pressure at mean sea level.

Modelling the engine power below the critical altitude should be quite straightforward since the engine power remains approximately constant. Above the critical altitude the engine power is mimicking the normally aspirated engine power. As the compressor cannot maintain the constant pressure above the critical altitude, and surrounding pressure is dropping with standard lapse rate, it is assumed that the power will drop with the same rate as in normally aspirated engine.

However, this simple assumption does not take into consideration the fact that the compressors are limited with mass airflow and that they are rising the inlet air temperature, above the surrounding one, by compressing it. For that reason, simple normally aspirated engine model will not provide the correct results, as the model should be quite simple and usable across all force induction engines.

For that reason, the pre-charged engine's power is modelled as shown below.

Equation 39: Pre-charged engine power model

$$P = P_{ISA,MSL} \cdot \sigma_{ISA,crit}^x \sqrt{\frac{T_{ISA}}{T}} \text{ [W]}$$

Equation 40: Sigma critical in standard atmospheric conditions

$$\sigma_{ISA,crit} = \frac{\rho_{ISA}}{\rho_{ISA,crit}}$$

Equation 41: Power model power factor

$$x = \log_{\sigma_{ISA,crit}} \frac{P}{P_{ISA,MSL} \sqrt{\frac{T_{ISA}}{T}}}$$

As the forced induced engines have a few more variables in comparison to normally aspirated engines, for the model it is necessary to introduce some new variables. One of them is density ratio in standard conditions with reference to density at a critical altitude. Power model power factor is a variable that is adjusted to every engine separately, and for its calculation it is required to know one maximum power setting above the critical altitude.

Similarly as in normally aspirated engines, temperature correction for non-standard conditions should be done according carburettor air temperature, on in case of fuel injected engines, inlet air temperature. But as this temperature isn't available, outside air temperature is used with the presumption that correcting the power in this way won't cause big errors.

Diagrams below show the reference data compared to the model results for some pre-charged engines. Figure 13 presents the reference data together with the model results for the Lycoming TIO-540-AK1A which is installed on Cessna 182TC. Figure 14 shows the reference and model data for Lycoming TIO-540-AJ1A which can be found on Cessna 206TC.

As seen from the diagrams, the model assures the correct engine performance.

Power - Altitude Lycoming TIO-540-AK1A (C182TC)

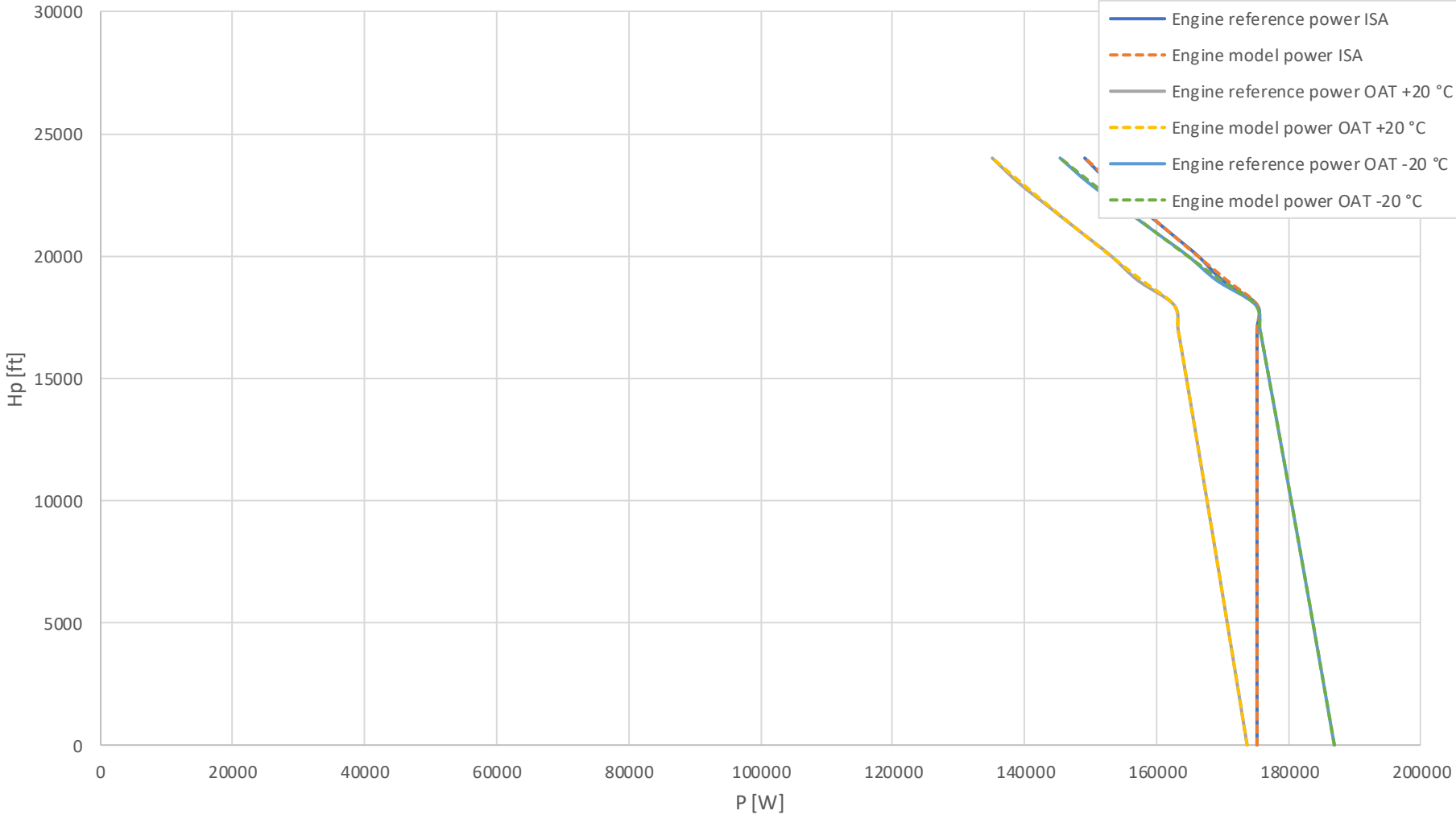


Figure 13: Power - Altitude graph for Lycoming TIO-540-AK1A (C182TC)

Power - Altitude Lycoming TIO-540-AJ1A (C206TC)

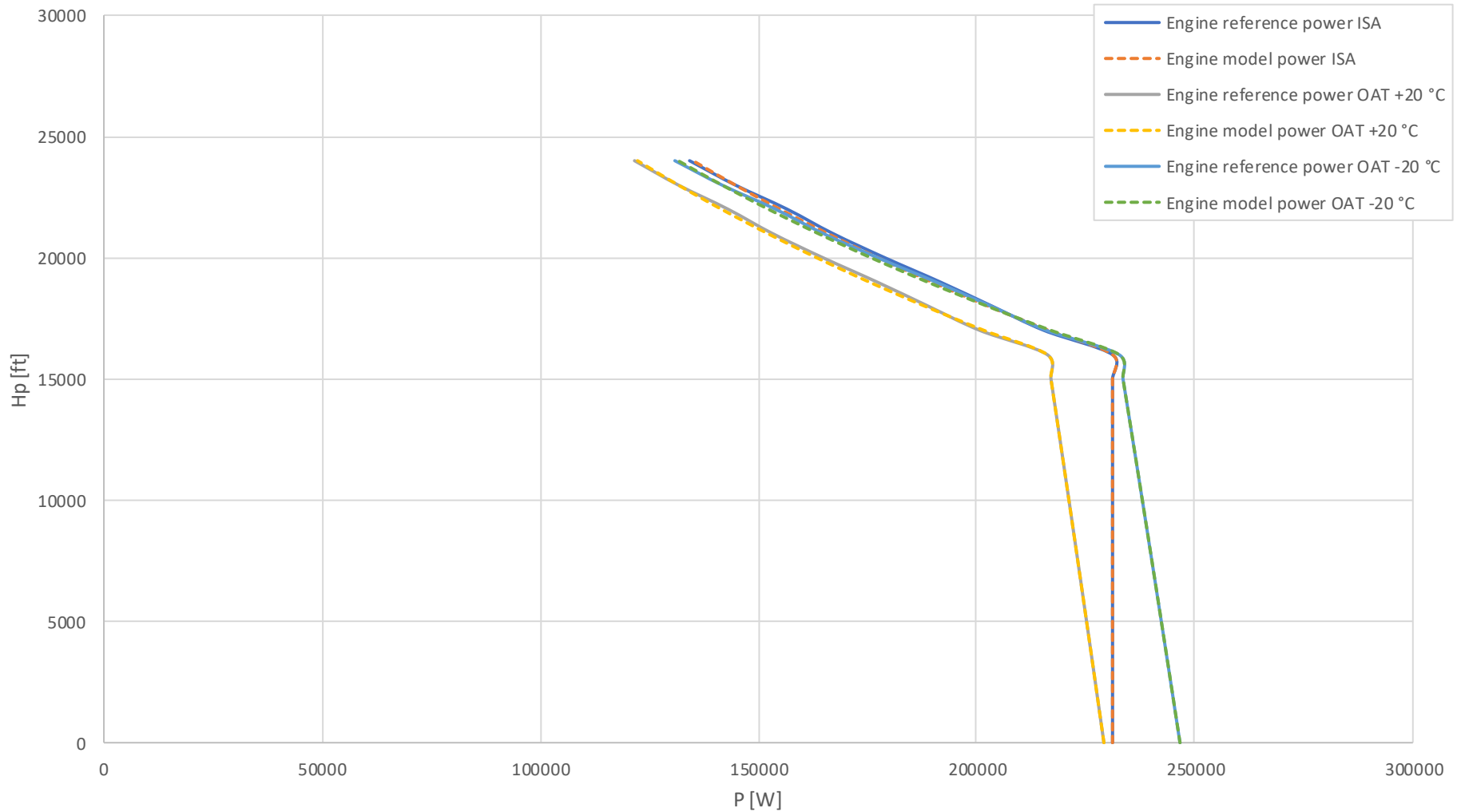


Figure 14: Power - Altitude graph for Lycoming TIO-540-AJ1A (C206TC)

3.2. Propeller efficiency model

Propeller is a device that converts engine's rotational energy into propulsive force. It operates in nearly the same way as an aircraft wing. Aircraft's wing produces lift by moving through the air by a certain speed which is a result of an aircraft thrust while the propeller is moved through the air by its rotation which is supplied by the engine. It is positioned in such a way that the resulting aerodynamic force is propelling the aircraft in forward motion.

As a wing compared to the airfoil has some losses, the propeller also has a certain efficiency. This efficiency is a ratio of thrust power produced by the propeller and engine power transferred to the propeller. Thrust power is a power used to produce the thrust of the propeller, every other power consumption is considered unwanted and by that premise it doesn't participate in efficiency calculation.

Equation 42: Thrust power

$$P_T = P \cdot \eta_{prop}$$

Equation 43: Thrust

$$F_T = \frac{P_T}{v_{TAS}}$$

As seen from the equation above, the propeller efficiency is important factor which shouldn't be forgotten in any calculations.

Two types of the propeller can be found on the airplanes, first one is the one which has a fixed pitch, and the other has a variable pitch. Propellers with fixed pitch are much simpler in construction and easier to operate but can't maintain good efficiency through different flight phases. They are usually pitched in such a way to operate efficiently around certain airspeed and certain rotational speed at higher altitudes. Variable pitch propellers are more complicated in construction, but allow maintaining set rotational speed, which allows to maintain the good propeller efficiency through various airspeeds. They are controlled in such a way that the propeller pitch is increased with increase in airspeed and power, and reduced with decrease in airspeed and power.

Modelling of the efficiency will have to be done separately for these two types of propellers.

3.2.1. Fixed pitch propeller efficiency

Fixed pitch propellers introduce new problem into modelling the propeller efficiency as their efficiency is dependent on the propeller rotation speed and airplane's velocity. Both of these values depend on the engine power, which again changes significantly with the change of the rotational speed, which depends on the propeller. This leads to the loop, in which the variables required for the calculation of the efficiency depend on each other. This calculation would require an iterative approach to determine only one efficiency value. An iterative approach to calculation in simulations is unwanted due to the fact that every simulation is based on many calculations, and adding unnecessary iterative calculations to it would cause a heavy load on computers.

For this reason, a method which can provide certain variables that would ensue a simple and concise calculation of the fixed pitch propeller efficiency would be preferred. Cubic spline method provides the ability to determine the fixed pitch propeller efficiency based on a three data points available in the airplane manual [5].

To include the limitation of the power and engine rotational speed to the model this method is slightly modified.

Before the efficiency calculation, it is required to determine at which altitude the airplane's engine can develop maximum rotational speed with fully open throttle. Fixed pitch propellers are usually pitched in that way so that they allow maximum rpm at an altitude where the maximum cruise power is obtainable. For example, Cessna 172 has 75 % power suggested as maximum cruise power, and highest altitude at which this power can be achieved is around 8000 ft. This is the reason why this altitude is chosen for the following calculations, while the maximum efficiency can be changed arbitrarily until the resulting efficiency matches the one needed to achieve the cruise and climb data in the aircraft manual.

As a first data point, it uses a maximum static thrust value determined by the following formula.

Equation 44: Static thrust

$$F_{Tstatic} = 0.85 \cdot P^{2/3} \cdot (2 \cdot \rho \cdot S_{prop})^{1/3} \cdot \left(1 - \frac{S_{spinner}}{S_{prop}}\right)$$

Second data point is a cruise data point, where the maximum propeller efficiency is assumed.

Equation 45: Cruise thrust

$$F_{TC} = \eta_{max} \cdot P / v_c$$

For the third point it is required to understand the change in maximum thrust with change in airspeed. As the airspeed increases from zero, the maximum thrust becomes smaller, implying that at any airspeed the maximum thrust will be smaller than the maximum static thrust. With the increase in airspeed the drop in thrust with airspeed becomes small until a certain point it starts to increase again. This change in maximum thrust with airspeed can be seen in the Figure 15.

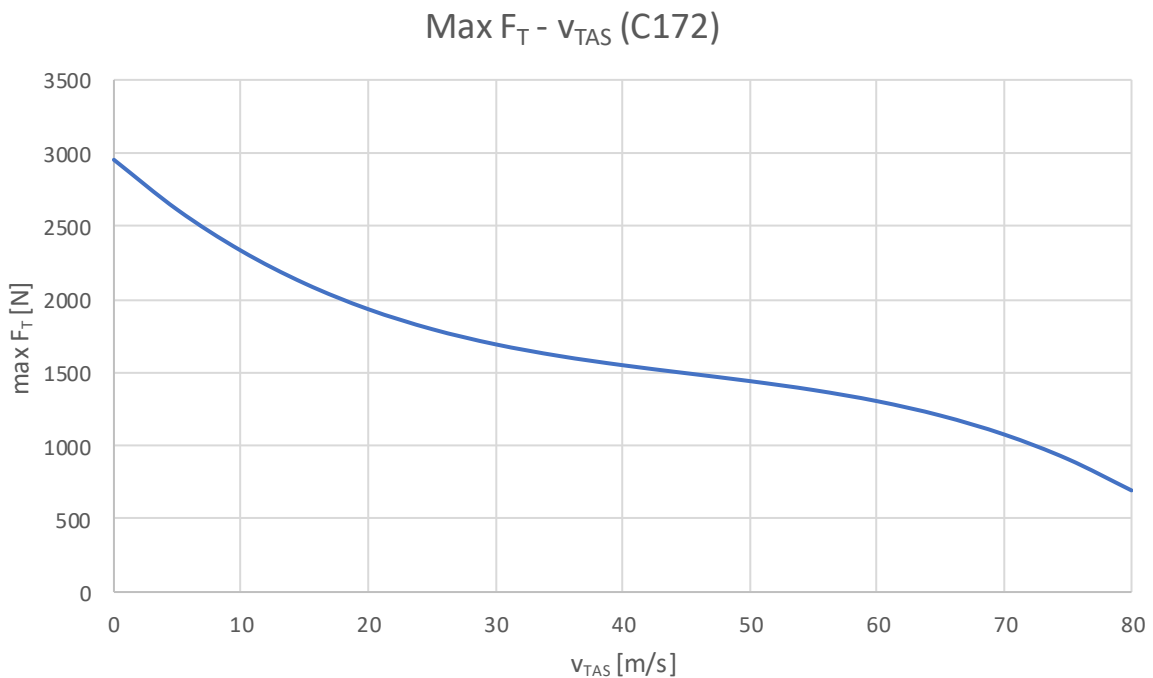


Figure 15: Maximum thrust – Airspeed graph for Cessna 172

Third data point used in this method for fixed pitch propeller is a point at which the drop in thrust with airspeed is at its minimum. This is optimized for the cruise, and the third equation can be derived from that.

Equation 46: Maximum efficiency point

$$\left(\frac{dF_T}{dv}\right)_{v_c} = \frac{-\eta \cdot P}{v_c^2}$$

And, the last data point used in this fixed pitch propeller efficiency model is a point with the highest airspeed.

Equation 47: Highest airspeed thrust

$$F_{TH} = \frac{\eta \cdot P}{v_H}$$

As stated earlier, engine power cannot be determined easily because it greatly depends on the rotational speed, for that reason these data points are taken in relation with the highest altitude at which the engine propeller combination can develop maximum rotational speed.

With this available data, the following calculation can be made.

Equation 48: Fixed pitch propeller efficiency matrix

$$\begin{bmatrix} 0 & 0 & 0 & 1 \\ v_c^3 & v_c^2 & v_c & 1 \\ 3 \cdot v_c^2 & 2 \cdot v_c & 1 & 0 \\ v_H^3 & v_H^2 & v_H & 1 \end{bmatrix} \begin{bmatrix} A \\ B \\ C \\ D \end{bmatrix} = \begin{bmatrix} F_{Tstatic} \\ F_{TC} \\ -\eta_P \cdot P / v_c^2 \\ F_{TH} \end{bmatrix}$$

Equation 49: Fixed pitch propeller efficiency coefficients

$$\begin{bmatrix} A \\ B \\ C \\ D \end{bmatrix} = \begin{bmatrix} 0 & 0 & 0 & 1 \\ v_c^3 & v_c^2 & v_c & 1 \\ 3 \cdot v_c^2 & 2 \cdot v_c & 1 & 0 \\ v_H^3 & v_H^2 & v_H & 1 \end{bmatrix}^{-1} \begin{bmatrix} F_{Tstatic} \\ F_{TC} \\ -\eta_P \cdot P / v_c^2 \\ F_{TH} \end{bmatrix}$$

Result from this matrix equation are four coefficients A, B, C and D which are used to calculate the thrust in flight for the certain airspeed.

Equation 50: Cubic spline thrust

$$F_T(v) = A \cdot v^3 + B \cdot v^2 + C \cdot v + D$$

With the following data it is possible to calculate the fixed propeller efficiency for the various advance ratio values as seen in Table 1. An example of the fixed pitch propeller efficiency can be seen in the Figure 16, where the coefficients obtained from the matrix are used to calculate the thrust and efficiency.

Equation 51: Fixed pitch propeller efficiency

$$\eta = \frac{F_T(v) \cdot v}{P}$$

Table 1: Fixed pitch propeller efficiency for Cessna 172

J	F _T (8000 ft)	η (8000 ft)
0,00	2954	0,00
0,12	2332	0,26
0,24	1933	0,43
0,30	1797	0,50
0,36	1693	0,56
0,45	1579	0,66
0,46	1565	0,67
0,48	1550	0,69
0,48	1548	0,69
0,53	1495	0,74
0,59	1441	0,80
0,65	1380	0,84
0,71	1304	0,87
0,75	1253	0,87
0,87	977	0,79
1,01	426	0,40

Propeller efficiency - fixed pitch propeller (C172)

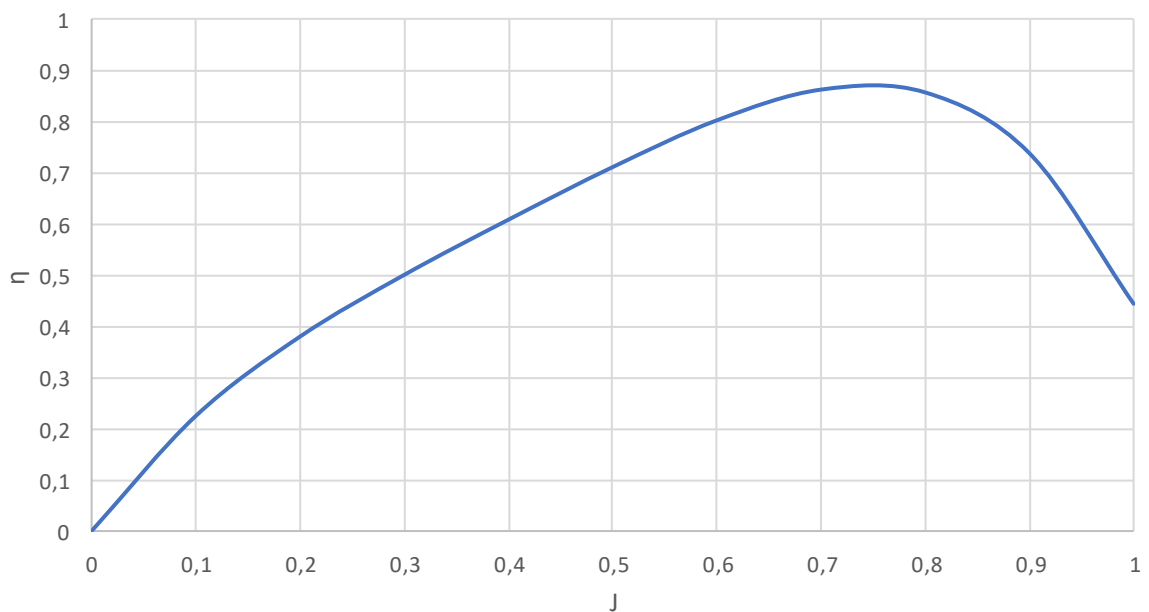


Figure 16: Propeller efficiency graph for Cessna 172

3.2.2. Variable pitch propeller efficiency

The construction and mode of operation of the variable pitch propeller allows it to maintain nearly constant high efficiency through various speeds and power settings.

Analysis of the propeller can be done by numerous methods, all of them have their advantages and disadvantages. For the variable pitch propeller efficiency, the momentum theory provides satisfactory results. The initial BADA 4 propeller efficiency is based on momentum theory, which results are confirmed by approaching the efficiency problem with different calculation method. In that sense, for the propeller efficiency, all following calculations are based on the initial BADA 4 model.

The momentum theory is a mathematical model of the propeller efficiency which assumes the following conditions [5]:

- the propeller is replaced by thin disc that offers no resistance to air passing through it
- the propeller disc is evenly loaded, which results in uniform flow through it
- the control volume surrounds the stream tube completely and separates the flow through the disc from the surrounding air
- surrounding air has a constant stagnation pressure (no work is applied on the surrounding air)
- far enough in front and behind the disc the streamlines are parallel and the stagnation pressure is equal to the surrounding air
- the propeller disc doesn't induce rotation to the flow
- the theory assumes inviscid and incompressible flow

The following equation represents the initial BADA 4 model of the propeller efficiency [3].

Equation 52: Variable pitch propeller efficiency

$$\eta = 2 \cdot \eta_{max} \left(1 + \left[1 + 2 \cdot \eta \frac{\dot{W}_P}{n_{eng}} \left\{ \sigma \cdot \rho_0 \cdot D_P^2 \frac{\pi}{4} v_{TAS}^3 \right\}^{-1} \right]^{\frac{1}{2}} \right)^{-1}$$

Obtaining the propeller efficiency from the previously listed propeller efficiency equation is possible by following the calculation steps in Appendix A. All the required variables are found in the aircraft manual, with exception to η_{max} which is chosen arbitrarily until the required power for horizontal flight, or for climb is same as the power obtained from the engine model.

An example of the propeller efficiency model result is a following graph which shows the resulting propeller efficiency for the given propeller advancement factor. Calculations for the propeller which can be found on the Cessna 182 can be seen in Figure 17.

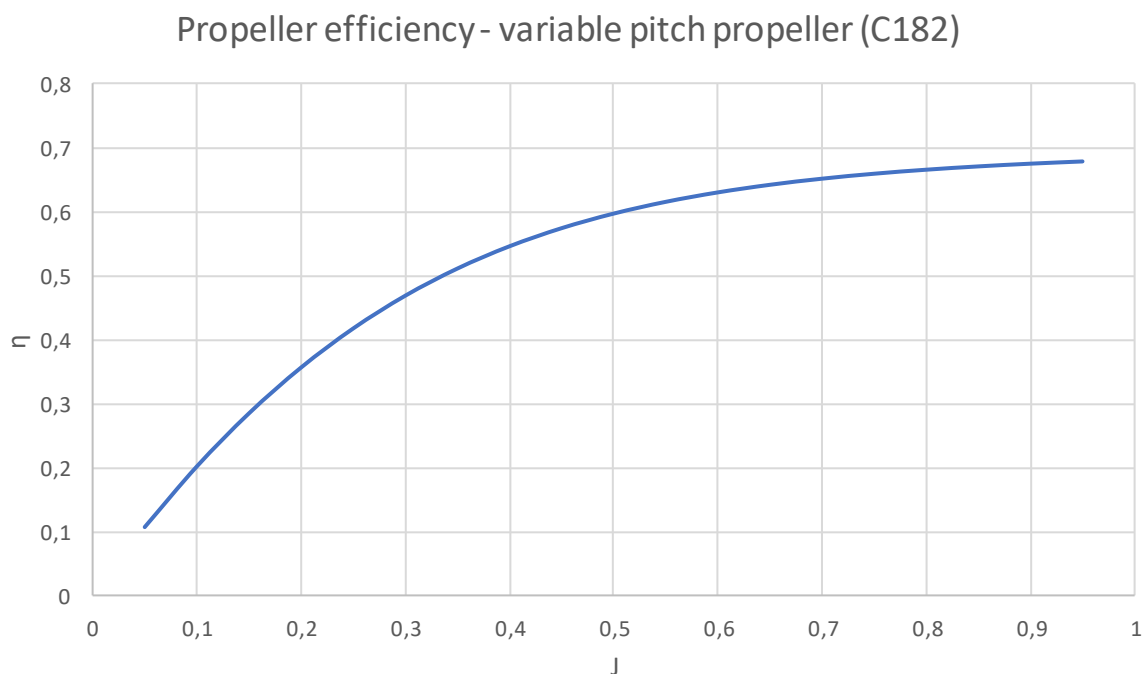


Figure 17: Propeller efficiency graph for Cessna 182

3.3. Drag polar

The initial BADA 4 model contained rudimentary drag polar obtained solely from climb performance data. As most general aviation airplanes often in their manuals only offer the best rate of climb performance data, obtaining the drag polar coefficients from this data would be quite imprecise. This can be explained by the simple fact that the best rate of climb lift coefficient and corresponding drag coefficient are constant, in other words, only one combination of lift coefficient and drag coefficients offer the best rate of climb performance.

The best rate of climb performance is achieved at a speed at which the maximum surplus of power is available. The maximum available power of the engine isn't dependent on the airspeed, while the power required to fly horizontally is. This means that the maximum surplus of power is located at a speed at which the required power is minimal. This speed is denoted as v_y , the best rate of climb speed.

As all general aviation aircraft only append climb performance data at this airspeed, acquisition of the drag polar coefficients from this data would be, as previously described, imprecise.

For this reason, it is necessary to obtain drag coefficients from other sources.

Additional problem for obtaining the drag coefficients from cruise data, is that the engine power model can vary due to the effect of the carburettor air temperature, which is often different from the outside air temperature. This can result in variation of power available. One other problem which cannot be solved easily is the difference between the engine power before and after engine installation in the aircraft. As airplane manufacturers do not describe this in their manuals, it can be assumed, again with a certain reserve, that the installed power is the same to the engine power obtained on the test bench. This of course introduces certain error in the calculation.

It is important to note that in propeller driven airplanes drag coefficients obtained from one flight condition, for example cruise, cannot be extended to other flight conditions, for example climb or descent [6]. This is due to the fact that in different flight conditions airplanes operate at different airspeeds and power settings, which can lead to significant changes in

slipstream effect on aircraft fuselage and wings. Slipstream effect is more noticeable on multi engine aircraft, especially in single engine operations [6], while one engine is inoperative, the other engine needs to produce more power and thrust, thus creating an even bigger torque. With all that said, at the moment the current BADA model will not assume any faults on the aircraft in flight.

Taking all the above in consideration, the initial drag coefficients will be extracted from the cruise performance data, as this data is available from the same source as climb performance data, and the possible error in drag coefficients can be mitigated later in the modelling process. Extracting drag coefficients from cruise provides a better range of power settings, as the cruise performance tables provide exact power percentages of nominal power. This is convenient as it is possible to separate this calculation from the engine model, with only one remaining variable as propeller efficiency.

For the extraction of drag coefficients from the available data two methods can be used. First method is quite straight forward, as the forces acting on aircraft in cruise are in balance, we can assume that the thrust is equal to the drag, and that the lift is equal to the weight. From those expressions we can derive the multiple lift drag combinations and extract the parasitic and induced coefficients for the drag. The second method is known as PIW-VIW method which is a test method used to reduce the data to the standard atmospheric conditions and standard aircraft mass, as our available data is already presented for standard conditions and at a standard mass, only the part for the drag coefficient extraction is used.

Both of the methods have their advantages and disadvantages. First method is very flexible in terms of additional lift and drag coefficients, and other modifications, but it is long in calculation for every point. The PIW-VIW method is quite concise and straight forward, but doesn't offer the flexibility and modification options as the first method. If the number of lift and drag coefficients is kept as standard, both methods provide the same result, but in any other case it is necessary to have an insight into wanted result to know which one is providing the correct result.

Some aircraft required the symmetric drag polar modelling for the successful integration into the performance model, while the other aircraft required an asymmetric drag polar.

Calculation process for the first method is done by using the formulas listed below.

Equation 53: Drag coefficient

$$c_D = \frac{2 \cdot P \cdot \eta}{\rho \cdot S \cdot v_{TAS}^3}$$

Equation 54: Lift coefficient

$$c_L = \frac{2 \cdot m \cdot g_0}{\rho \cdot S \cdot v_{TAS}^2}$$

After obtaining the drag and lift coefficients, from the cruise performance data, for the multiple altitude, power setting and airspeed combinations, the relationship between the stated is determined by method of linear regression.

Equation 55: Drag lift relationship

$$c_D = \frac{c_L^2}{\pi \cdot e \cdot AR} + c_{D0}$$

Equation 56: Drag lift relationship

$$c_D = c_{D2} \cdot c_L^2 + c_{D0}$$

Example of this can be seen below in Figure 19, as done for the Cessna 182.

Calculation process of the second method is shown below.

Equation 57: PIW factor

$$PIW = \frac{P \cdot \eta \cdot \sqrt{\sigma}}{\left(\frac{F_G}{F_{Gstd}}\right)^{\frac{3}{2}}}$$

Equation 58: VIW factor

$$VIW = \frac{v_{TAS} \cdot \sqrt{\sigma}}{\sqrt{\frac{F_G}{F_{Gstd}}}}$$

After obtaining multiple PIW -VIW combination points, linear regression method is applied to determine the relationship between the PIW·VIW and VIW⁴ factors. This can be seen on Figure 20 as done for the Cessna 182 airplane.

After determining the relationship of the PIW·VIW and VIW⁴ the following formulas are used to determine the parasitic and induced drag coefficients.

Equation 59: Parasitic drag coefficient

$$c_{D0} = \frac{k \cdot 2}{S \cdot \rho_0}$$

Equation 60: Induced drag coefficient

$$c_{D2} = \frac{l \cdot \rho_0 \cdot S}{2(m \cdot g_0)^2}$$

Expressions behind drag polars are stated below.

Equation 61: Symmetric drag polar

$$c_D = c_{D2} \cdot c_L^2 + c_{D0}$$

Equation 62: Asymmetric drag polar

$$c_D = c_{D2} \cdot (c_L - c_{LminD})^2 + c_{D0}$$

Figure 18 shows the polar for the Cessna 182 with appropriate climb and cruise points as an example. This polar is one of the main goals of this research, and data fit such as this one is very gratifying. It can be seen that both the cruise and climb points fit perfectly with the selected drag coefficients.

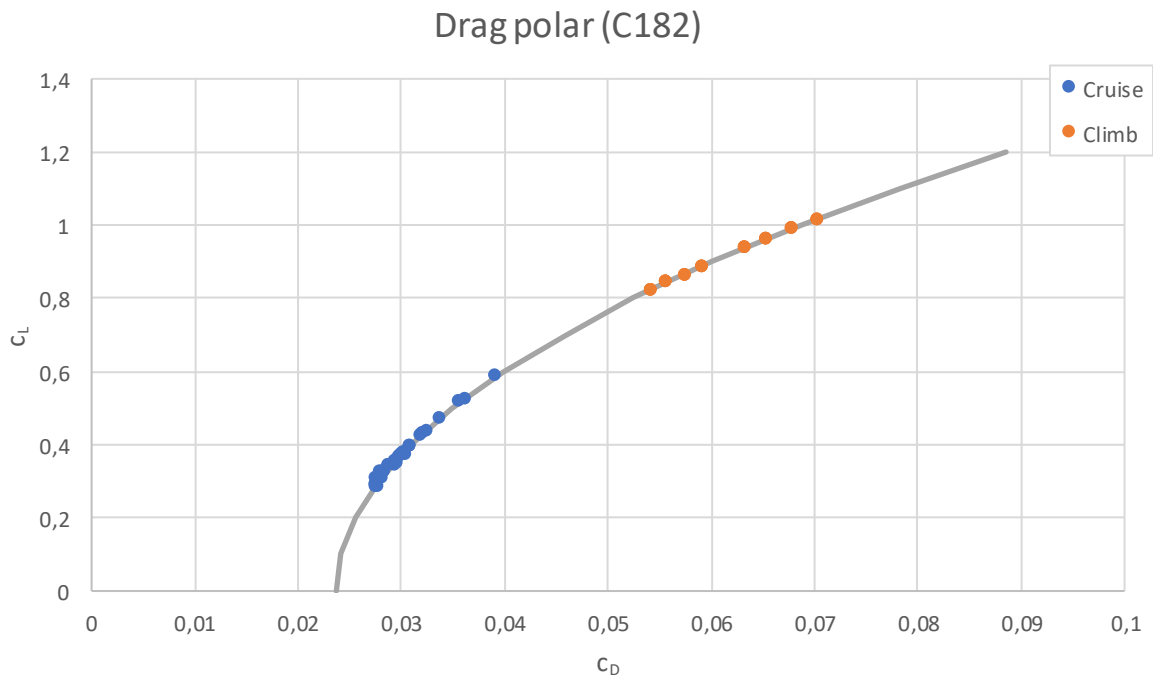


Figure 18: Polar for Cessna 182 with cruise and climb points

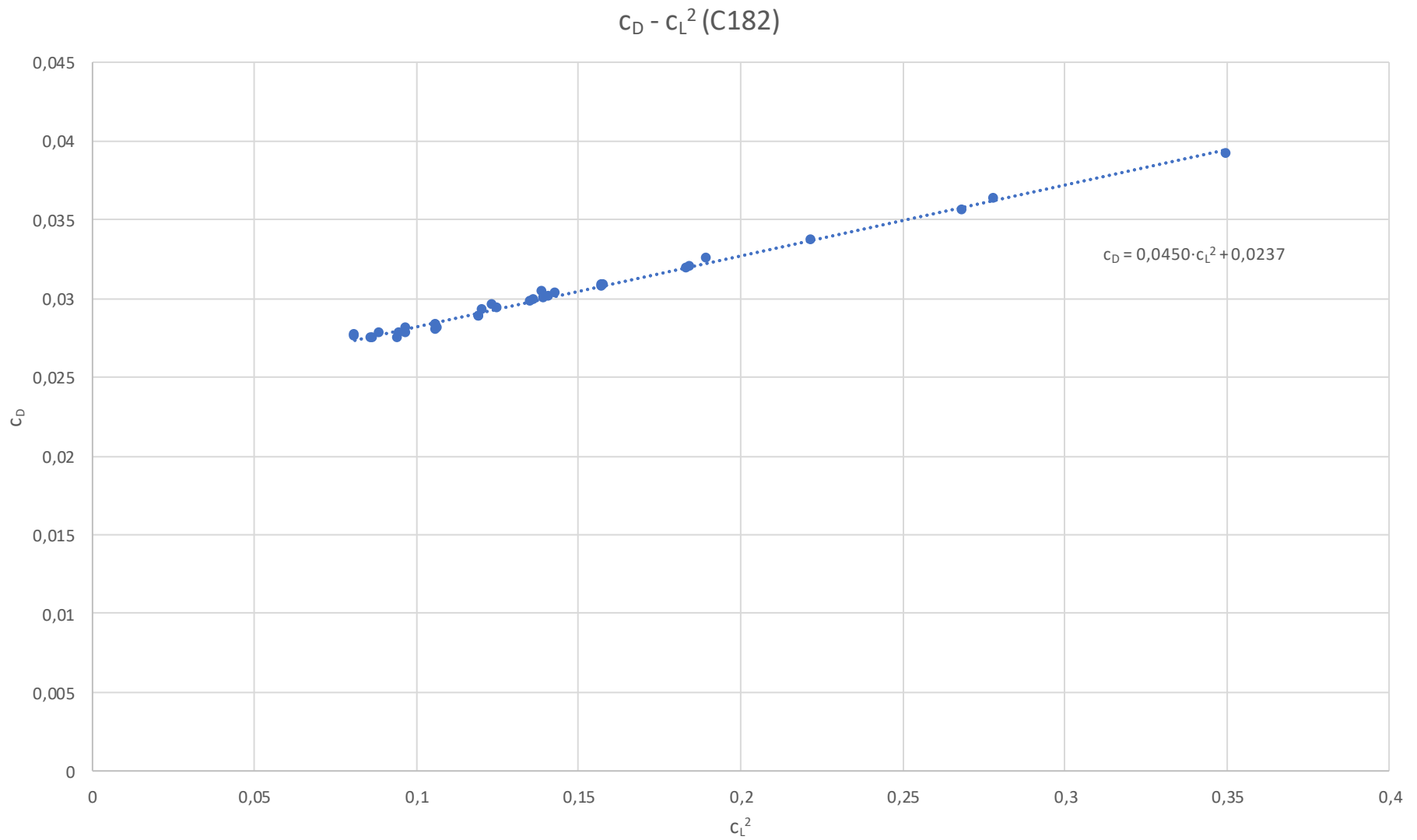


Figure 19: Linear regression of lift drag coefficient combination for Cessna 182

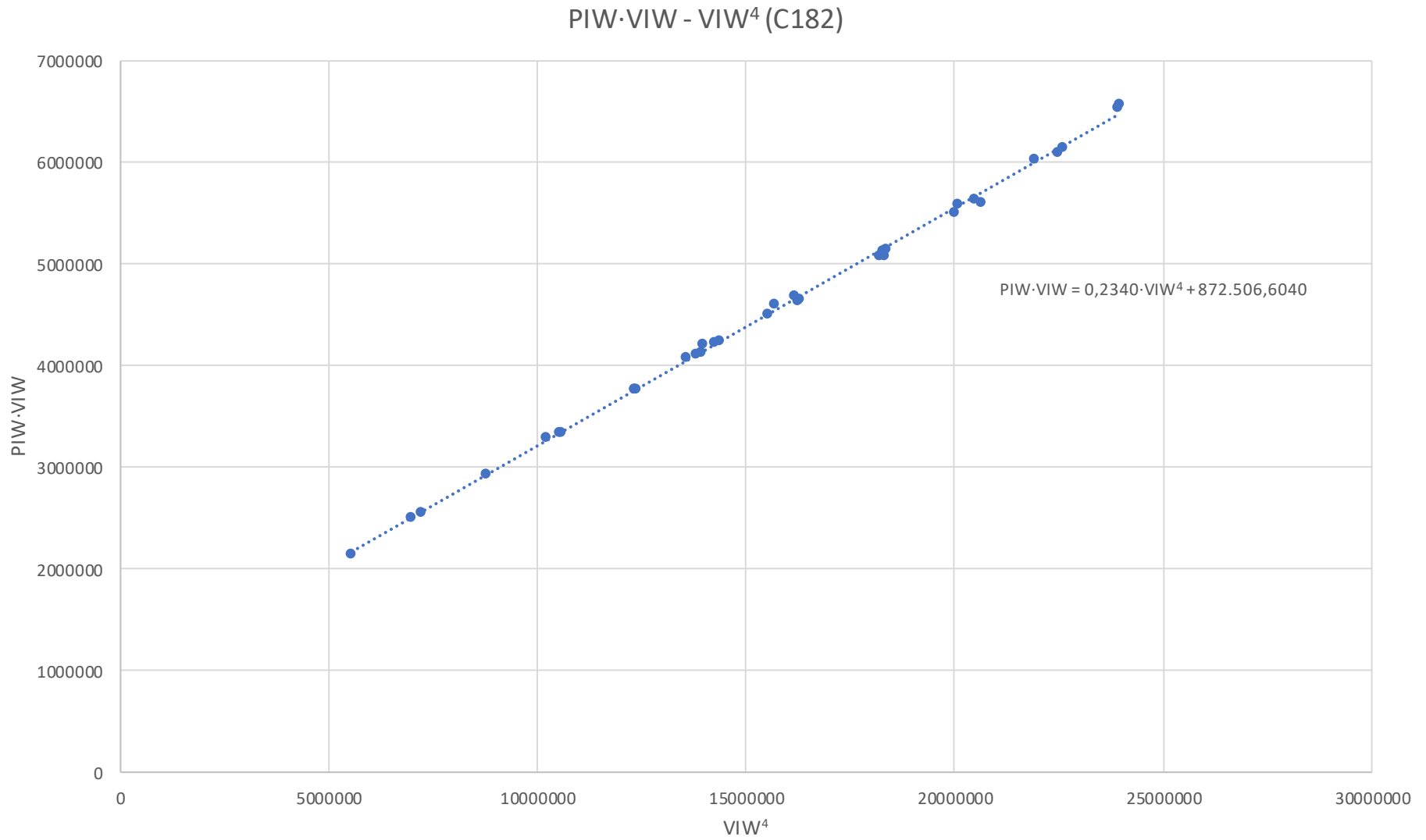


Figure 20: Linear regression of PIW·VIW VIW⁴ combination for Cessna 182

3.4. Vertical speed / Rate of Climb conversion

Most aircraft manufacturers provide climb performance data, for their aircraft, under the performance manual in their manuals. This data is most commonly presented in form of a table or a diagram, providing the rate of climb versus the altitude data for multiple masses or often only maximum takeoff mass, and for different temperature conditions.

In analysis of the initial BADA 4 model rate of climb data was taken directly from the aircraft manual without any additional manipulation.

To obtain this data, before aircraft certification, the airplane manufacturer conducts multiple flight tests. As a normal, atmospheric conditions during these flight tests aren't standard, and the measured values of rate of climb need to be processed, or reduced to obtain the values in standard and non-standard atmospheric conditions, also with regard of airplane's changing mass.

One of the available methods for this data reduction is called PIW-CIW. This method corrects the obtained data to the standard aircraft mass and standard atmospheric conditions. Included in this reduction method there is a correction for non-standard atmosphere temperature, which converts the measured value of rate of climb to vertical speed [7].

Using this method for data reduction implies that the data stated in the aircraft manual as climb performance is in fact vertical speed versus altitude, not rate of climb versus altitude as stated in most of the manuals.

To confirm this premise a simple flight test was in order, which would replicate the steps taken by the aircraft and aircraft manual manufacturer during their tests and data reduction methods. Details of the flight test can be found in chapter 5.5. As a result of this flight test it is concluded that the data provided in the aircraft manual as climb performance is indeed vertical speed versus altitude.

To account for this conclusion, a small temperature correction to the original manual data is required to convert it to the rate of climb, as the model is developed around the rate of climb value. Making this correction is much easier than adjusting the whole model to fit the new variable.

As stated already, a simple correction is required to obtain the rate of climb value from the vertical speed. This correction can be seen below.

Equation 63: Vertical speed / Rate of Climb conversion

$$ROCD = v_v \frac{T_{ISA}}{T} \text{ [ft/min]}$$

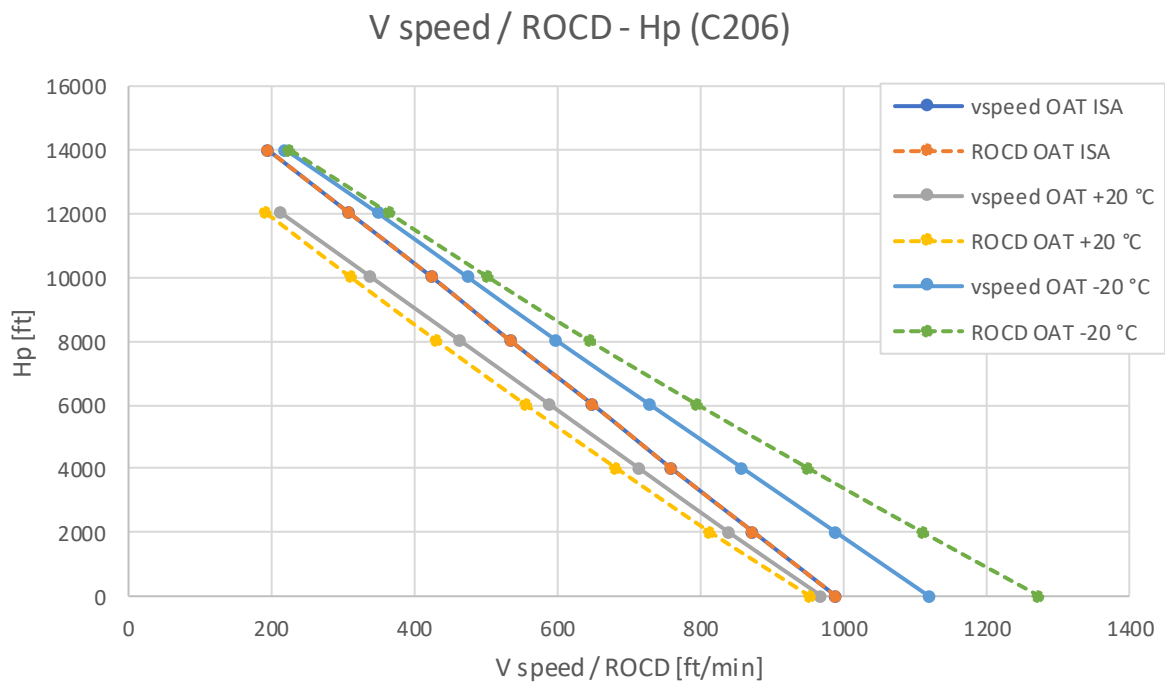


Figure 21: Vertical speed / Rate of Climb comparison at different altitudes and temperatures graph for Cessna 206

Difference between the values of vertical speed and rate of climb can be observed in the Figure 21, as the values are related to a Cessna 206 airplane.

4. Analysis of the improved model segments

In this chapter all the model improvements will be analysed separately. By that means, each improvement will be added on top of existing model to try and determine the overall improvement of the model.

The improvement will be shown as a graph, for the easement of interpretation. On this graph, there will be two values shown, one will represent the airplane's required power to climb at a rate of climb published in the airplane's manual for a certain atmospheric condition. The other value will be the engine power model which represents the maximum available power, modelled according to the engines operating manual.

By simply comparing the two values it is possible to determine how good the airplane performance model follows the values stated in the airplane's manual.

For example, in the following subchapters the Cessna 182 aircraft will be used, except for the fixed pitch propeller efficiency where the Cessna 172 aircraft will be used.

4.1. Engine performance model

The engine performance model doesn't have a direct impact on the model, it just provides the necessary reference that the performance model uses. This reference is the maximum power available versus altitude, and this can be seen in chapter 3.1. Following figures show the same performance model but different with different reference power models.

Figure 22 shows the improved engine model in standard conditions, the difference between the already existing model and the new model are not big, at least not in standard conditions, but this brings a more precise and reliable reference to the modelling process.

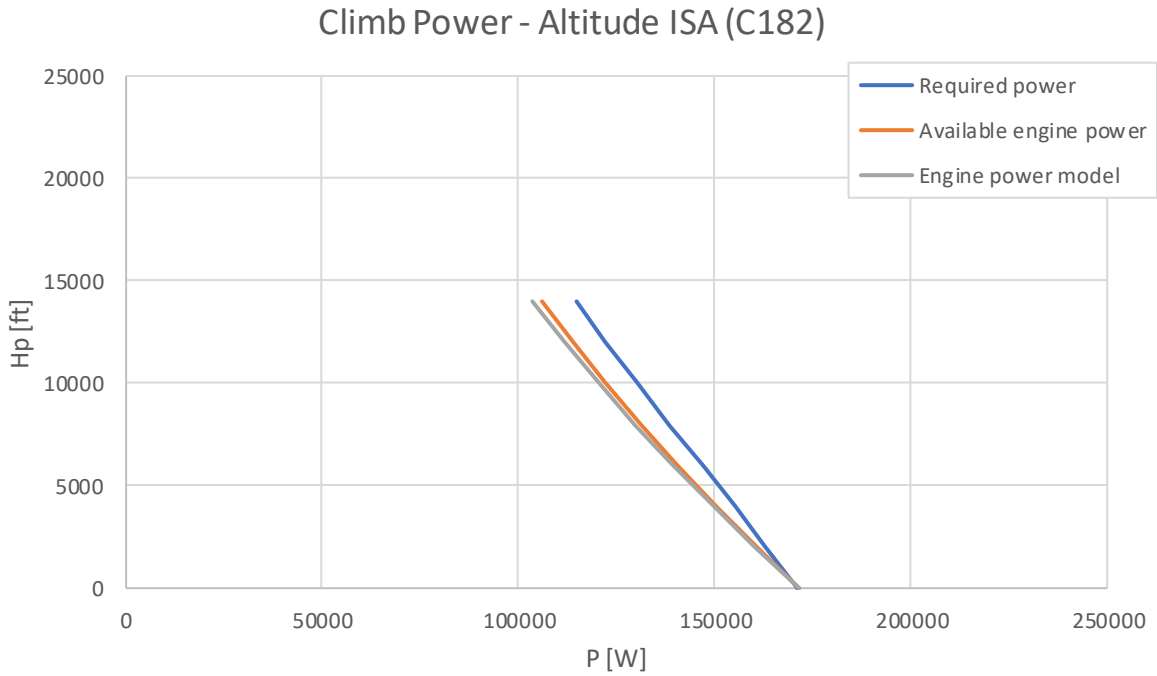


Figure 22: Climb Power - Altitude ISA graph for Cessna 182

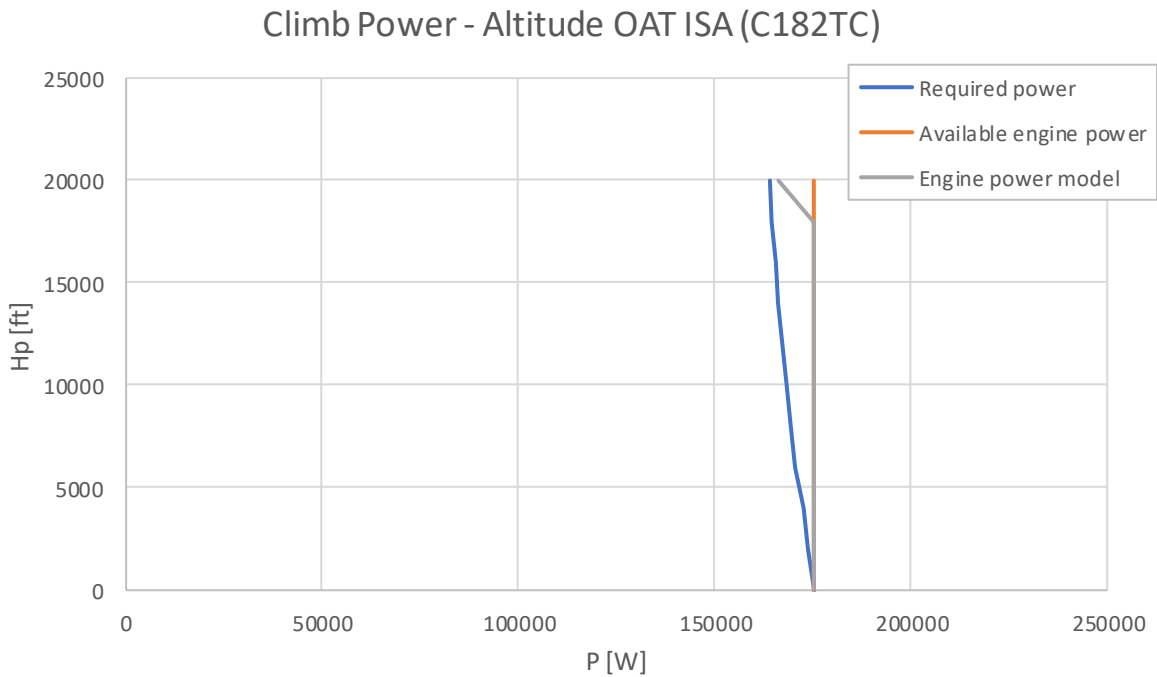


Figure 23: Climb Power - Altitude ISA graph for Cessna 182 TC

Figure 23 represents the improved engine model, in standard atmospheric conditions, for the turbocharged engine in Cessna 182 TC. However, from the shown data, it is clear that the engine power model won't provide the best fit to the reference climb power data available

from the airplane's manual. In the manual there is no visible performance loss border at critical altitude, which means that the engine after the installation in aircraft, particularly in climb data, has different power than the one tested on the test bench. The power is lower and there is no sharp altitude border above which the performance loss is greater.

4.2. Propeller efficiency model

Fixed pitch propeller efficiency model is a new model added to the performance model.

Variable pitch propeller efficiency was already correct and as that, the verification of it doesn't impose any change to the performance model. For that reason, the change in performance model for this segment doesn't exist and won't be show as an improvement in this section.

4.3. Drag polar

Correct determination of drag coefficients, improves the performance model drastically. As drag coefficients are quite small in value, it is required to determine the precisely.

The result of accurate determination of drag coefficients can be seen in Figure 24.

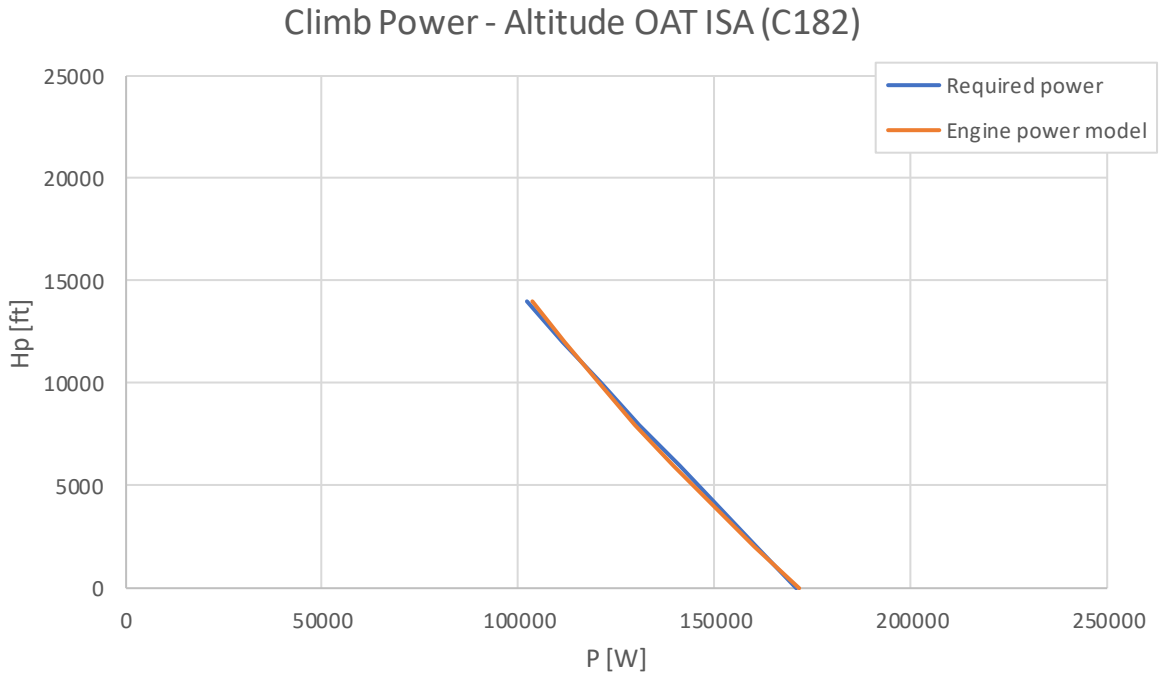


Figure 24: Climb Power - Altitude OAT ISA graph for Cessna 182

At this point, the required power of the aircraft to climb with maximum rate of climb at a certain altitude, coincides with the engine power model. This is only observable in standard atmospheric conditions.

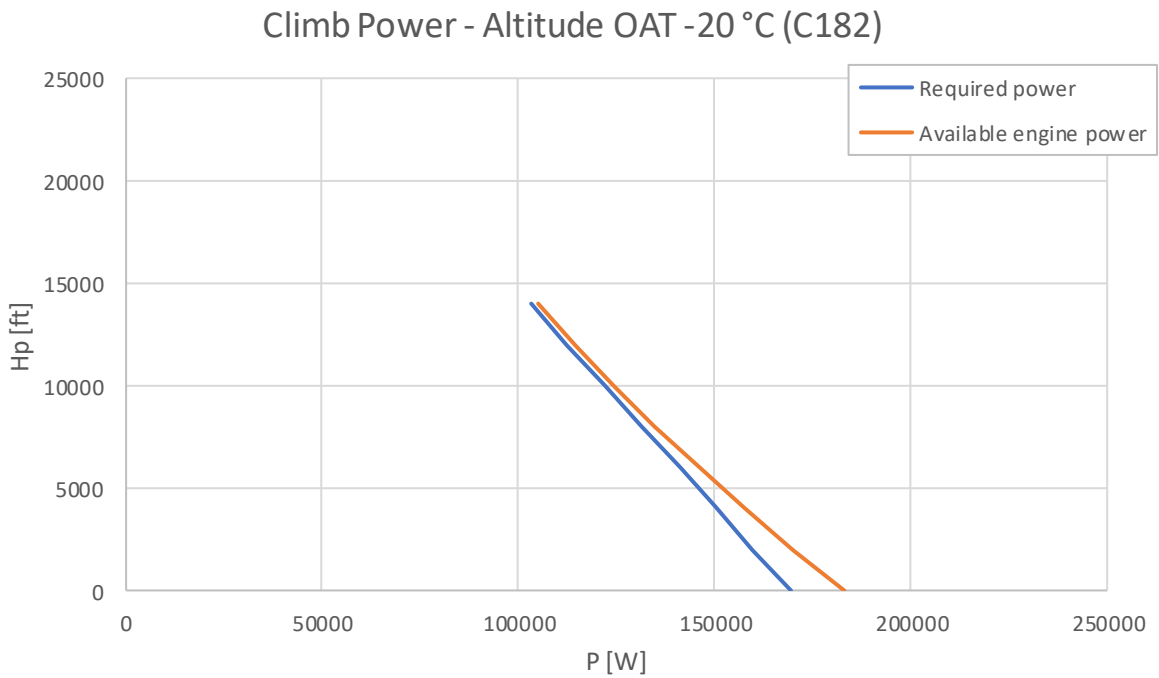


Figure 25: Climb Power - Altitude OAT -20 °C graph for Cessna 182

Figure 25 and Figure 26 still show a considerable difference in power requirement and available power, for that reason it is safe to assume that there exists another temperature correction which isn't accounted for. This is solved in section 3.4.

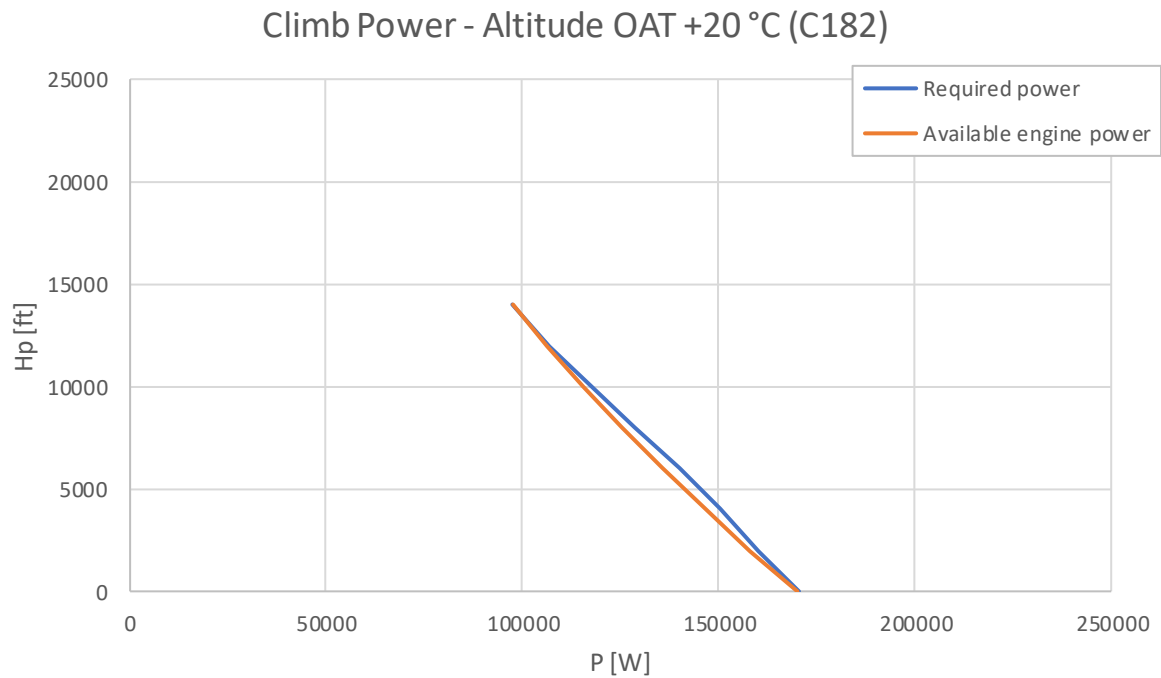


Figure 26: Climb Power - Altitude OAT +20 °C graph for Cessna 182

4.4. Vertical speed / Rate of climb conversion

This conversion is necessary due to the method that is used for data reduction after the flight tests used by the manufacturer to populate and publish the corresponding aircraft manuals.

Vertical speed to rate of climb conversion doesn't have an impact on standard atmospheric conditions values, but only to the non-standard conditions.

Figure 27 and Figure 28 represent the power available to climb at published rates through various altitudes in non-standard conditions, and serve as a reference to see how much does vertical speed to rate of climb conversion improve the results in non-standard conditions.

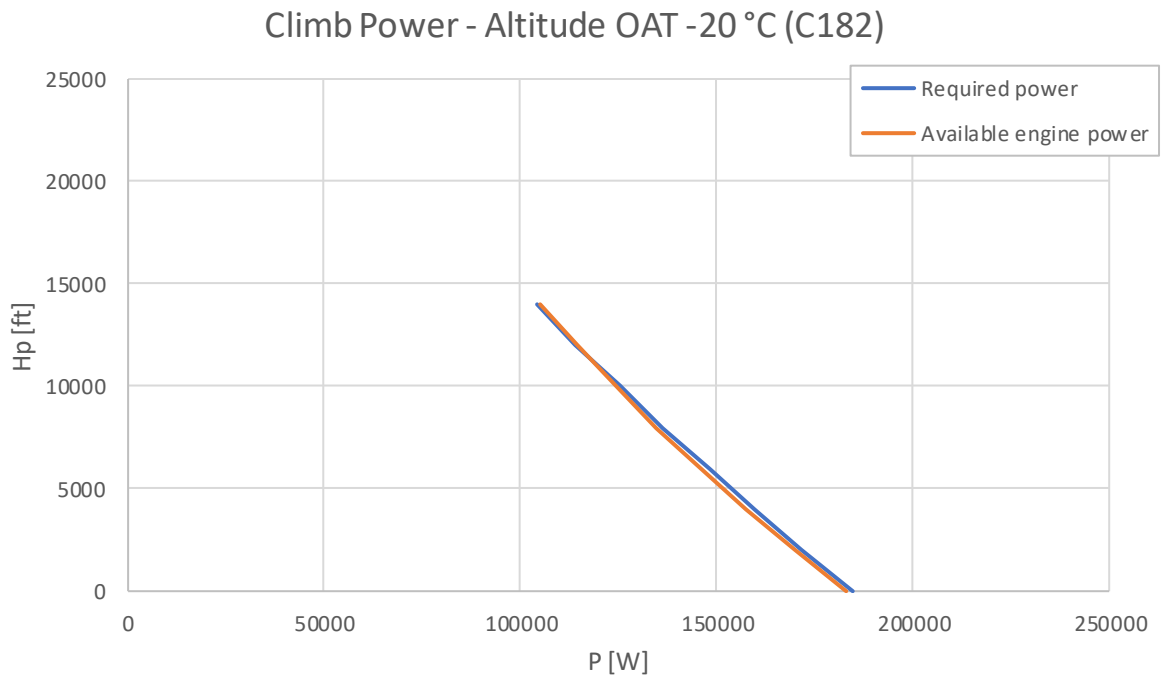


Figure 27: Climb Power - Altitude OAT -20 °C graph for Cessna 182 without vertical speed conversion

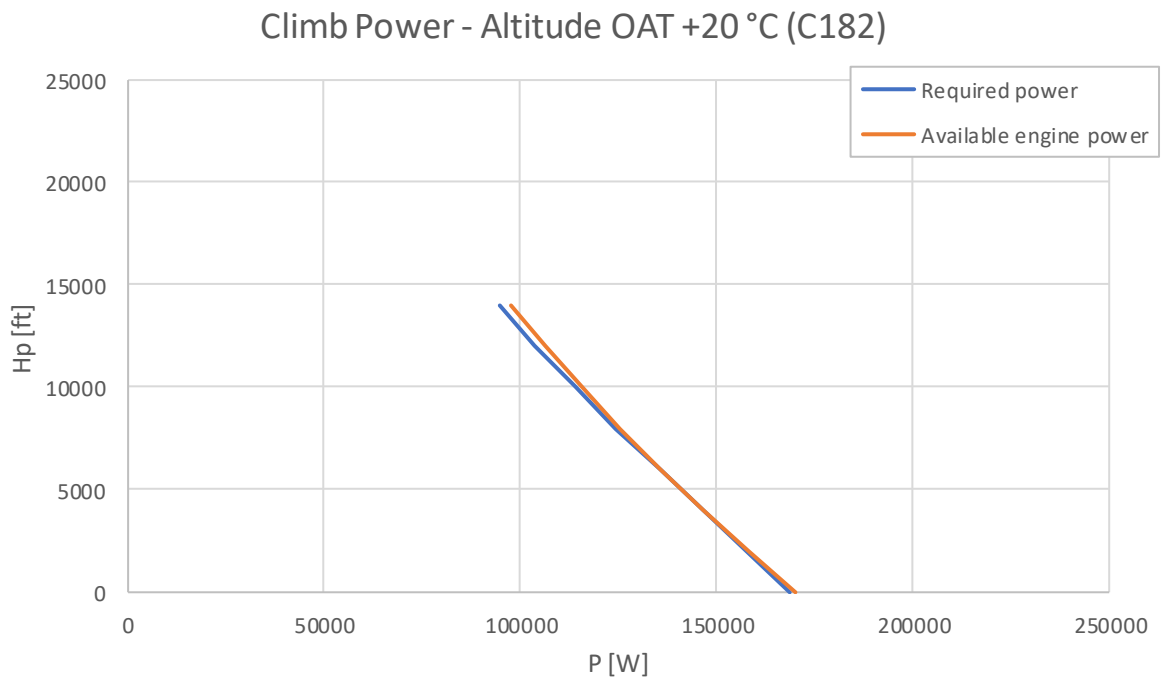


Figure 28: Climb Power - Altitude OAT +20 °C graph for Cessna 182 without vertical speed conversion

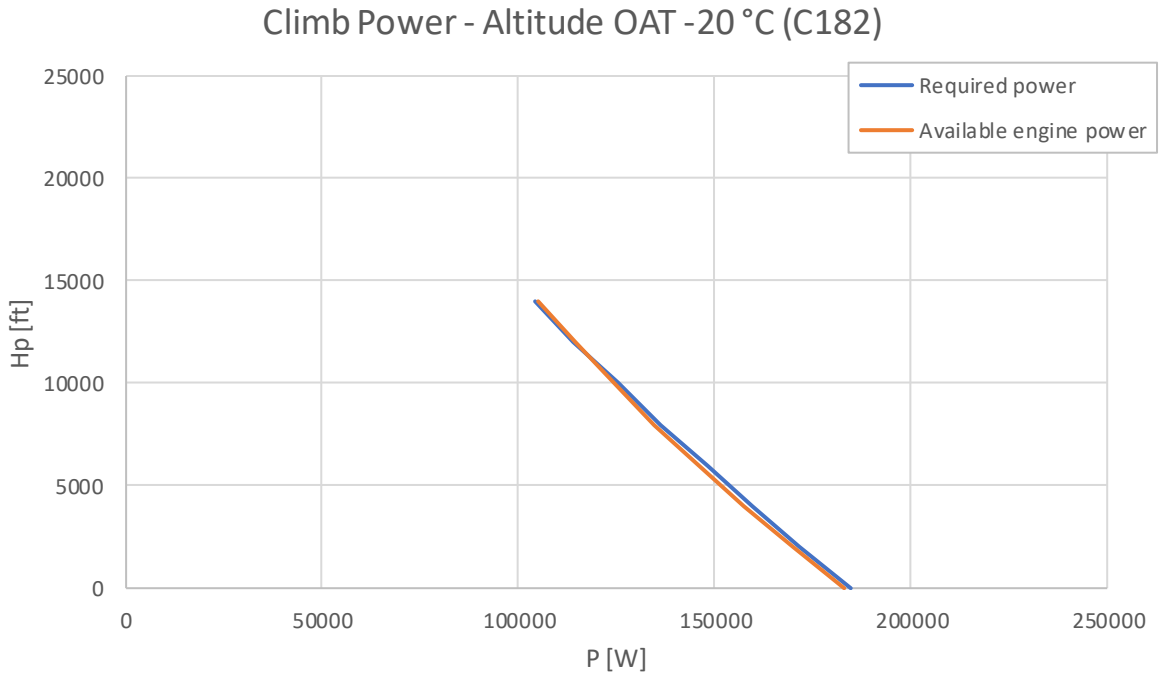


Figure 29: Climb Power - Altitude OAT -20 °C graph for Cessna 182

Figure 29 and Figure 30 show the required power coinciding with the available engine power in non-standard atmospheric conditions.

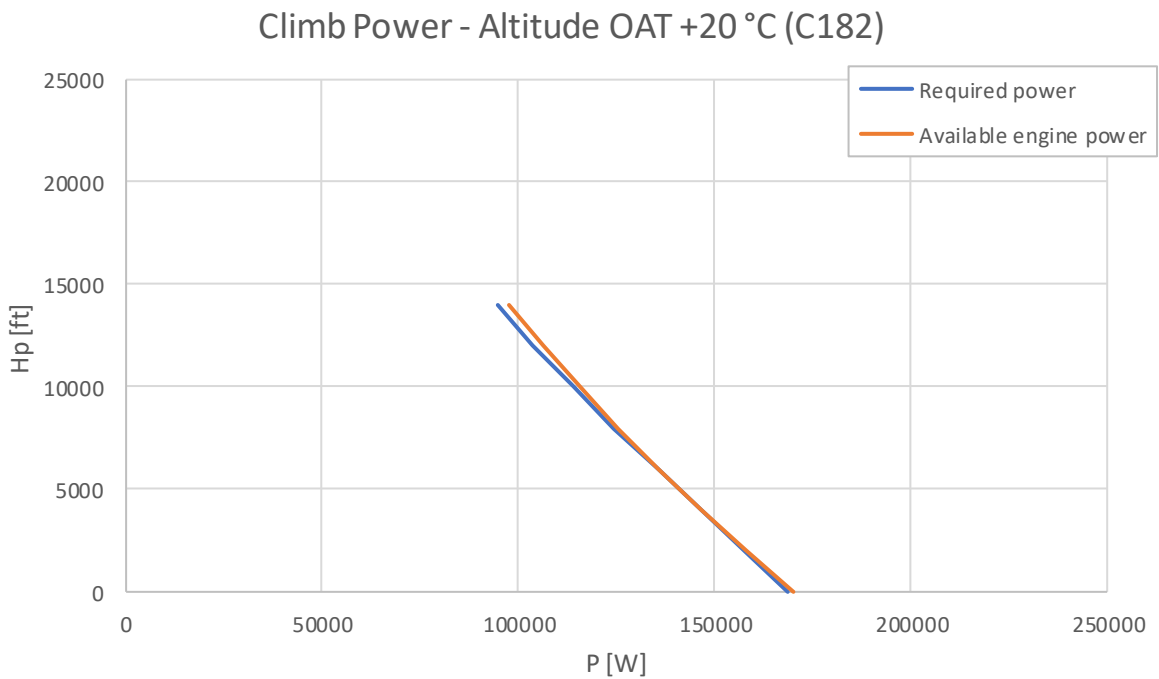


Figure 30: Climb Power - Altitude OAT +20 °C graph for Cessna 182

4.5. Summary of the improved segments

To better represent the overall improvements to the model result, the result are calculated with the usage of all the segments and the results can be compared to the values stated in the manual.

Two important values that can be compared are climb vertical speeds, and cruise speeds.

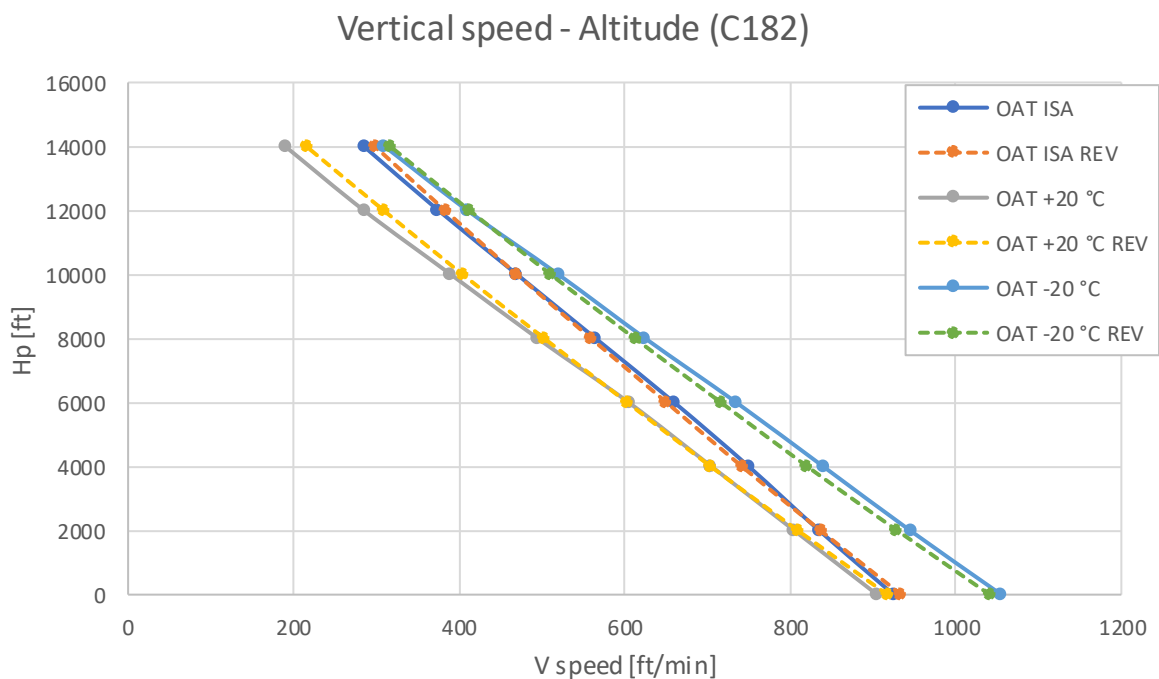


Figure 31: Vertical speed - Altitude graph for Cessna 182

Figure 31 shows the model result compared to the values obtained from the airplane's manual. Values denoted as ISA, +20 and -20 are values obtained from the manual, while the values denoted as ISA REV, +20 REV, and -20 REV are the values obtained as model results. At this point, the modelling process was reversed, and the data obtained is a result of combined proposed improvements. Data represents the maximum obtainable vertical speed in steady climb. This is done by providing the model with the best rate of climb speed, and everything else is a calculated as a part of model. As seen on the graph, the overall error in the model is negligible.

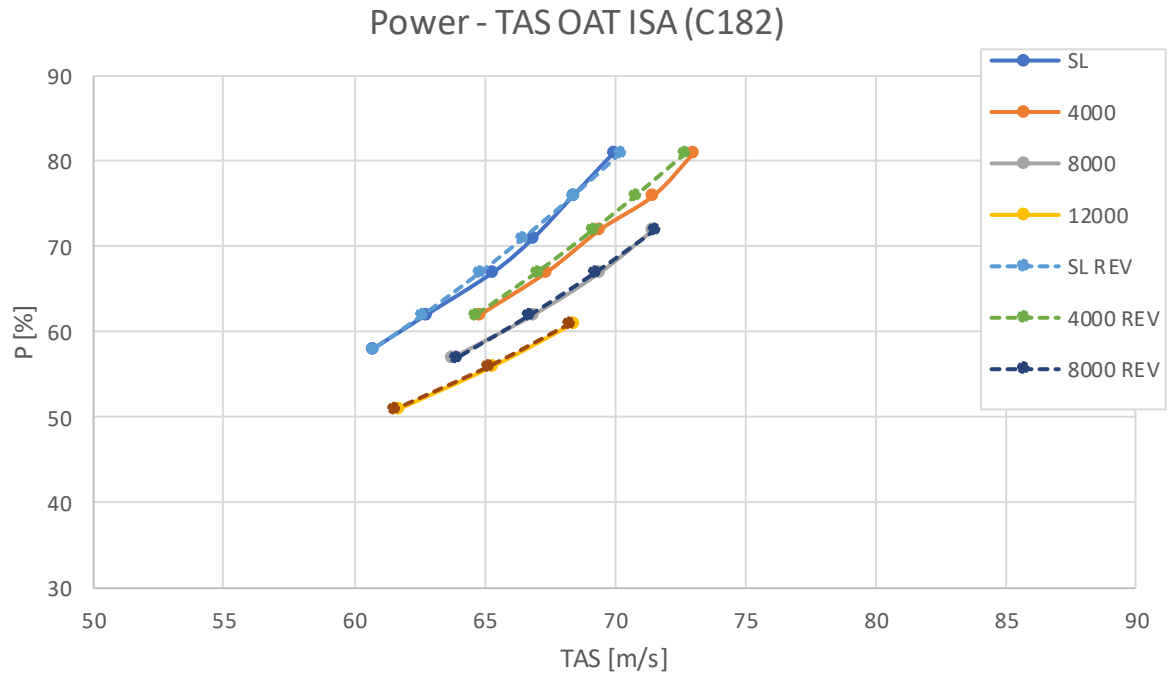


Figure 32: Power - True Airspeed OAT ISA graph for Cessna 182

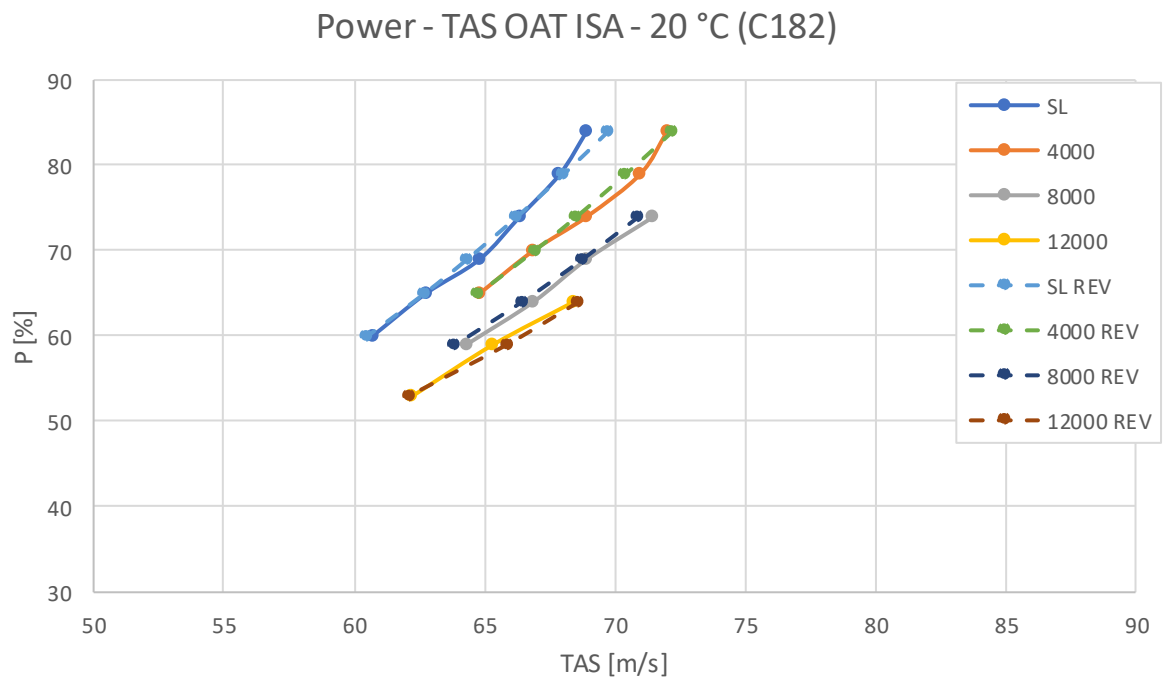


Figure 33: Power - True Airspeed OAT -20 °C graph for Cessna 182

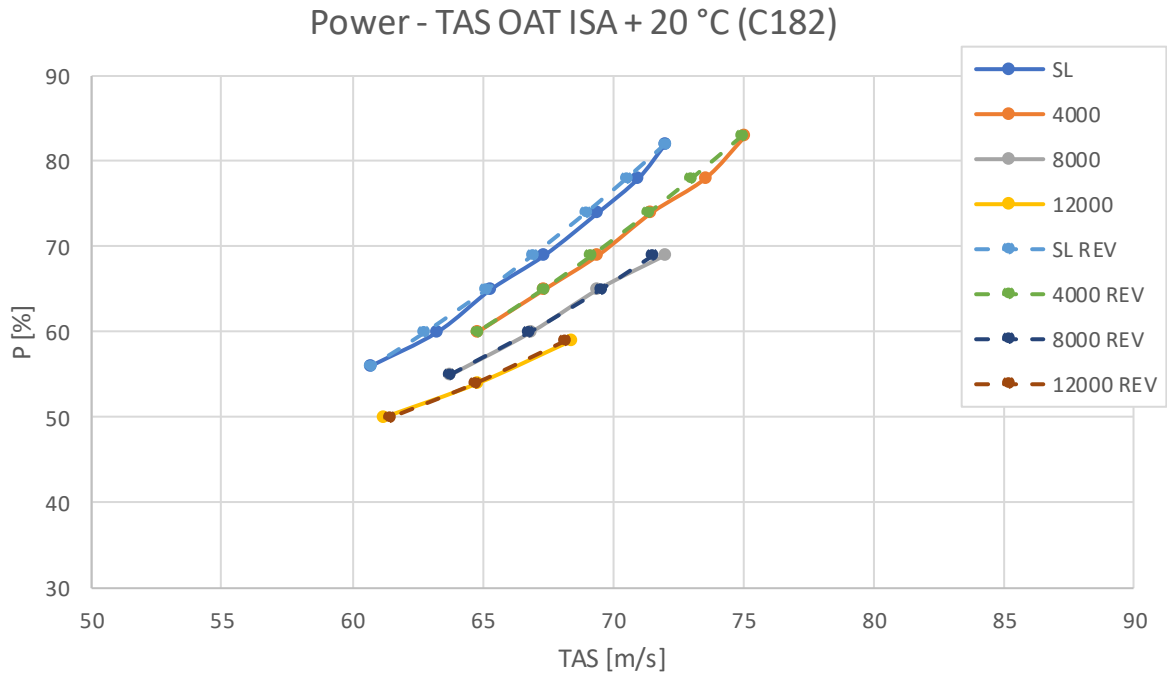


Figure 34: Power - True Airspeed OAT +20 °C graph for Cessna 182

Figure 32, Figure 33 and Figure 34 show performance model results, cruise true airspeed, in comparison with the data obtained from the cruise performance section in the airplane's manual. Model results were obtained by reversing the process of determining the cruise drag coefficients, and using the force balance to determine the speed of the aircraft in cruise. The airspeed is maximum obtainable with chosen power setting. Results from the model are satisfactory as a relatively small mistake, presented as difference between the model results and manual data, can be explained as a rounding of airspeed values both in airplane's manual and in model calculation process.

5. Flight tests

Flight test is one of the available tools for checking aircraft performance. For complete understanding and interpretation of available aircraft performance data, extrapolated from the airplane flight manuals and aircraft engine performance manuals, it is necessary to determine the integrity of available data. Using this data, with reference to altitude and air temperature, it is possible to model aircraft performance accurately.

During the certification of aircraft, manufacturer is obligated to test its performance and provide the following in the airplane flight manual. All of these tests are greatly affected by the conditions in which they are conducted. For all non-standard conditions, as outside air temperature, winds, aircraft mass and position of centre of gravity, as well as airplane instability in flight during the tests.

With the following tests some published performance data is checked for its integrity, and some data is recorded for future calculations as it isn't listed in airplane flight manual.

5.1. Flight test segments

Engine performance test is to compare the available engine power with that stated in the airplane flight manual. Test should be conducted as a climb with maximum engine power setting. And by climbing through the beforehand decided altitudes, the engine power setting should be recorded. Engine power setting is determined by its manifold absolute pressure (MAP), and revolutions per minute (RPM). With recorded data it is possible to determine the maximum available power of the engine, by using the engine performance manual.

Cruise performance test is to determine airplane's drag polar, subsequently its drag coefficients. Airplane's drag consists of parasite drag and induced drag. Parasite drag coefficient changes due to the attack angle of an aircraft, but these changes are small in value so this drag coefficient can be considered constant. Induced drag coefficient is greatly dependent on the airplane lift coefficient, which for horizontal stable flight is determined by

the airplane's mass and cruise speed. Using this knowledge and airplane's engine power setting, with the help of first test results, it is possible to determine these drag coefficients.

Climb performance test is used to determine airplane's maximum rate of climb through different altitudes and compare them to the ones stated in the airplane's flight manual. Climb performance is limited with the available power, coming from the engine, the required power, required to overcome drag of the airplane, and airplane's weight. Available power will be determined with the help of the airplane flight manual and results from the first test. Required power will be determined by the available data from the airplane flight manual and results from the second test. Airplane's weight will be calculated by following the timeline, engine power setting changes and by the airplane flight manual data.

Descent performance test is to determine engines fuel consumption in low power regimes, as most general aviation airplane's manuals don't contain this information.

5.2. Flight test conduction

Flight test should be conducted in a stable atmosphere. For that reason, the flight should take place in early morning hours.

Airplane's mass should be known through all the test points, for that reason aircraft is to be refuelled to maximum fuel capacity before the flight is to start. All crew should be weight before the test with all the gear that they are bringing into the aircraft. With the help of the timeline and aircraft flight manual, fuel consumption should be calculated at every engine power setting change in order to keep track of the fuel mass on the airplane. Some airplanes have engine monitoring computers installed, from which the data regarding the flight can be downloaded and used in a spreadsheet format, this alleviates the weight determining process. After conducting the flight, it is necessary to refuel the airplane and compare the fuel burn between calculated and measured value.

Engine performance test and airplane's climb performance can be conducted simultaneously as for the climb test the maximum power setting is required.

Airplane climb performance test should be conducted in a saw tooth pattern, which means that the airplane is to climb and descend through the same altitudes' multiple times. Few hundred feet below the beforehand determined altitude the airplane should begin its climb with maximum power and selected indicated airspeed. When the airplane is in stable flight, the timing should begin. After the airplane climbed through the selected altitude, and is above it by the same amount for which it was below it, when the timing started, the stopwatch should be stopped. After this the airplane can slowly descend back to the starting altitude, and begin the new cycle. This is done with the airplane configuration as stated in the airplane flight manual, for reference, and in every other desired configuration.

Cruise performance is to determine the airplane's drag polar. This is done by setting the desired engine power setting and stabilizing the airplane around certain airspeed, with the aim for rate of climb at zero. After the airplane stabilizes the engine power setting, its airspeed and mass should be noted, and from that data it is possible to calculate its drag coefficients.

Descent performance is to be tested in normal descends with different power settings. By adhering to one airspeed, the airplane's drag is constant, but its descent rate changes. Constant airspeed and drag help in determining the fuel flow in engines low power setting regimes. During descents predetermined power setting is to be set, and fuel flow noted, after that the second power setting can be used.

For all the test points atmospheric data should be known, as it is required to determine the results of the test, and to correct the results for standard conditions.

For the easy processing of the acquired data it is recommended that the flight is recorded with a video camera, particularly the instrument panel. With the recordings it is always possible to readdress the data and procedures.

It is recommended to prepare a certain checklist to be used before each test star in order to achieve and ensure same and constant conditions in flight test, and not to forget anything. In addition to the checklist it is a good practice to predetermine all the required variables and prepare the in a table form for the flight test.

5.3. Flight test data reduction methods

Different flight test data reduction methods exist, but eventually all of them offer same results for the collected flight test data. All of them serve a purpose of reducing the raw flight test data to standard values that are more representable and serve more than one set of conditions. Furthermore, these reduction methods offer a possibility to extend the flight test data beyond the measured ranges.

Various methods exist for various flight test regimes and flight phases, for that reason only the methods used in after these flight tests will be addressed, any other can be found elsewhere in literature.

5.3.1. PIW – VIW data reduction method

PIW – VIW methods is a method that derives the single power required curve for all airplane weights and all air densities. It draws a connection between the power and airspeed in level flight. One of the assumptions of these methods is that at a given angle of attack the lift and drag coefficients are constant. This leads to the appearance of the standard airspeed which is noted as VIW [7].

Equation 64: VIW factor source

$$\frac{F_{Gstd}}{F_{Gtest}} = \frac{F_{Lstd}}{F_{Ltest}} = \frac{c_L \frac{1}{2} \rho_{std} v_{std}^2 S}{c_L \frac{1}{2} \rho_{test} v_{test}^2 S}$$

Equation 65: VIW factor

$$VIW = \frac{v_{TAS} \sqrt{\sigma}}{\sqrt{\frac{m_{test}}{m_{std}}}}$$

By following the same assumption, the standard power can be determined similarly.

Equation 66: PIW factor source

$$\frac{F_{Tstd} v_{std}}{F_{Ttest} v_{test}} = \frac{F_{Dstd} v_{std}}{F_{Dtest} v_{test}} = \frac{c_D \frac{1}{2} \rho_{std} v_{std}^3 S}{c_D \frac{1}{2} \rho_{test} v_{test}^3 S}$$

Equation 67: PIW factor

$$PIW = \frac{P_{eng} \eta \sqrt{\sigma}}{\left(\frac{m_{test}}{m_{std}}\right)^{3/2}}$$

From this data it is possible to plot a curve which would represent the airplane's required power for a given airspeed.

To determine the airplane's drag coefficients, the process is the same as in chapter 3.3.

5.3.2. PIW – CIW data reduction method

PIW – CIW method is very similar to the PIW – VIW method. Instead of introducing standard airspeed, it is necessary to introduce the standard vertical speed. PIW factor is calculated in the same way as in PIW – VIW method.

Equation 68: PIW factor

$$PIW = \frac{P_{eng} \eta \sqrt{\sigma}}{\left(\frac{m_{test}}{m_{std}}\right)^{3/2}}$$

CIW, or standard vertical speed is calculated in the following way.

Equation 69: CIW factor

$$CIW = \frac{\left(\frac{dH_p}{dt}\right) \frac{T}{T_{ISA}} \sqrt{\sigma}}{\sqrt{\frac{m_{test}}{m_{std}}}}$$

Plotting the PIW – CIW diagram leads to a single line representing the vertical speed achievable by the certain power used.

To determine the vertical speed versus altitude, it is simply required to determine the vertical speed from the PIW – CIW diagram and plot it against the altitude.

Equation 70: Vertical speed from CIW

$$v_{speed} = \frac{CIW \sqrt{\frac{m}{m_{std}}}}{\sqrt{\sigma_{std}}} [ft/min]$$

5.3.3. PIW – NIW

PIW – NIW is an additional method, in which we can correlate rotational speed of a fixed pitch propeller to the engine power. This method is rarely used alone, but it can be used in order to exchange PIW in certain methods with NIW, and represent the reduced data on another level, which is maybe more easily understandable for some.

NIW parameter is a standard rotational speed, calculated in the following way.

Equation 71: NIW factor

$$NIW = \frac{rpm \sqrt{\sigma}}{\sqrt{\frac{m_{test}}{m_{std}}}}$$

By introducing this parameter to other methods, we then have NIW – VIW and NIW – CIW methods, which again are a blend of two methods.

5.4. Cessna Flight Test

Cessna 172 is very common general aviation airplane. It has a Lycoming engine paired with the fixed pitch propeller. This airplane was tested to confirm the available airplane's flight manual data, and to help in the modelling of the fixed pitch propeller efficiency.

For the flight test the Cessna 172, with the registration mark 9A-DMB, was used. Specifically, this airplane has an engine monitoring computer installed, which was a determining factor for descent performance test planning.

Flight test checklist for this set of flight tests and this airplane can be seen as Table 2.

Data sets for this flight test were obtained from airplane’s flight manual, and can be seen for their respective test segments as Table 3, Table 4 and Table 5.

Table 2: Cessna 172 flight test checklist

Cruise performance test	
Altimeter	STD (1013 hPa)
Altitude	As per table
Cabin ventilation	OPEN
Carburetor heat	OFF
Mixture	MAX RPM
RPM	As per table
Stabilize the airplane	
Climb performance test	
Altimeter	STD (1013 hPa)
Altitude	1000 ft below test altitude
Cabin ventilation	OPEN
Airspeed	As per table
Carburetor heat	OFF
Mixture	MAX RPM at test altitude
RPM	MAX PWR
Start the climb, stabilize the airplane	
Time from 500 ft below test altitude to 500 ft above test altitude	
RPM	NORM CRZ
Stabilize the airplane for cruise	
Descend with different power settings	

Table 3: Cessna 172 cruise performance test data set

Cruise performance test			
Hp [ft]		RPM	
4000	2100	2300	2500
6000	2100	2300	2500
8000	2200	2400	2600

Table 4: Cessna 172 climb performance test data set

Climb performance test				
Hp [ft]	Start IAS [kn]	Stop IAS [kn]	Increment [kn]	MROC IAS [kn]
4000	60	100	10	71
6000	60	100	10	70
8000	60	100	10	69

Table 5: Cessna 172 descent performance test data set

Descent performance test	
RPM	
	1200
	1300
	1400
	1500
	1600
	1700
	1800

Cruise performance test results are shown as $PIW \cdot VIW - VIW^4$ diagram in Figure 35, from which the following drag coefficients were obtained.

$$c_{D0} = 0,040927$$

$$c_{D2} = 0,113598$$

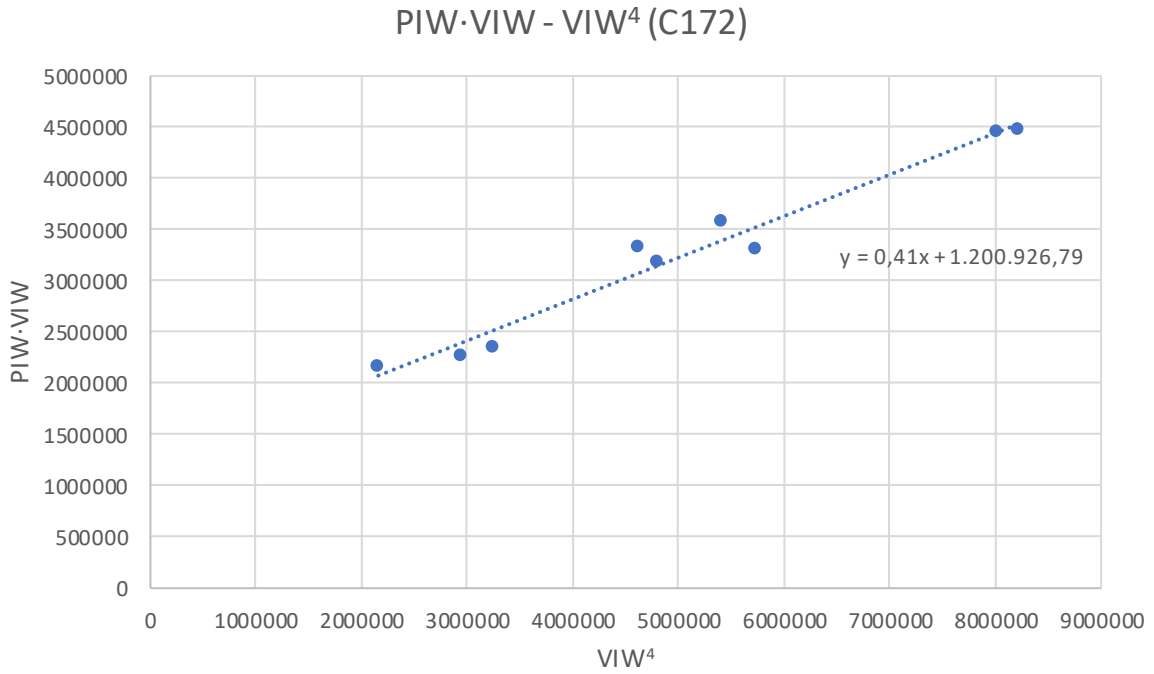


Figure 35: Cruise performance results for Cessna 172

Climb performance results are shown as PIW – CIW diagram in Figure 36.

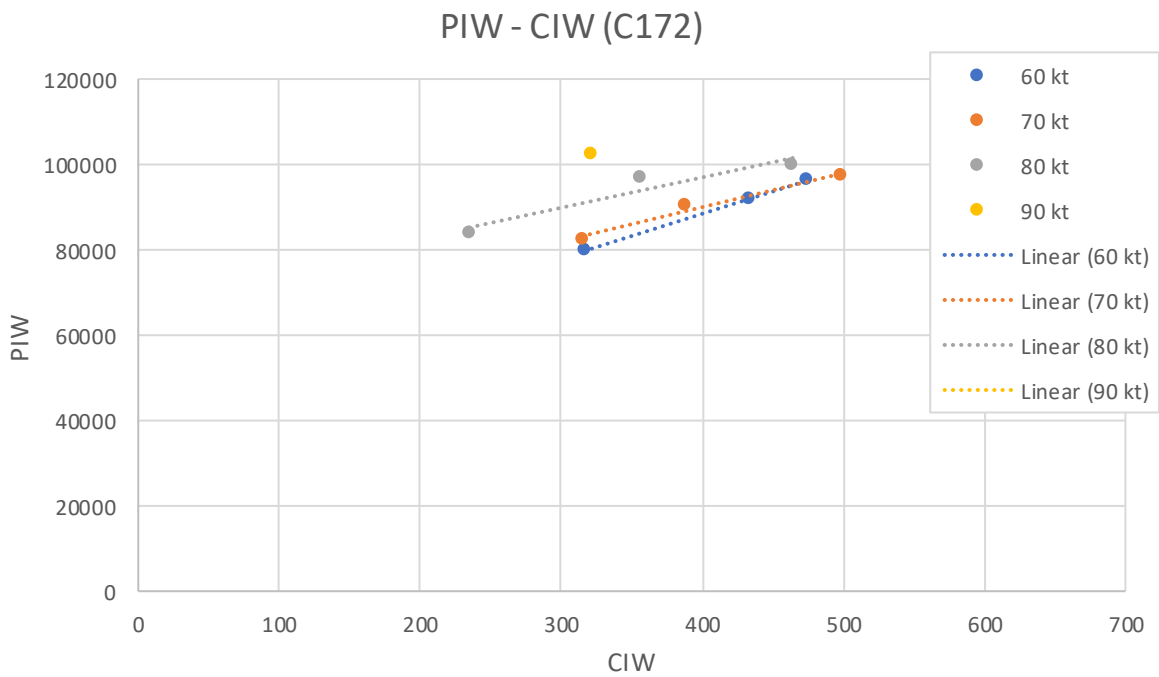


Figure 36: Climb performance results for Cessna 172

5.5. Diamond Flight Test

Diamond DV-20 is a small general aviation aircraft popular for its small fuel consumption figures. It has a Rotax 912 S engine paired with the variable pitch propeller.

For the flight test the Diamond DV-20, with the registration mark 9A-DIG, was used.

This airplane's manual lacks certain performance data and by some flight test segments it was intended to extrapolate these from the flight test.

Flight test checklist for these flight tests and this airplane can be seen as Table 6.

Table 6: Diamond DV-20 flight test checklist

Engine performance test	
Altimeter	STD (1013 hPa)
Altitude	As per table
Carburetor heat	OFF
RPM	FULL
MAP	FULL
Cruise performance test	
Altimeter	STD (1013 hPa)
Altitude	As per table
Cabin ventilation	OPEN
Carburetor heat	OFF
RPM	As per table
MAP	AS per table
Stabilize the airplane	
Climb performance test	
Altimeter	STD (1013 hPa)
Altitude	500 ft below low altitude limit
Cabin ventilation	OPEN
Airspeed	As per table
Flaps	As per table
Carburetor heat	OFF
RPM	2260
MAP	FULL
Start climb	
Stabilize the airplane below low altitude limit	
Climb	- 1 min, until high altitude limit
Power setting	NORM
Horizontal flight	
Descend to 500 ft below low altitude limit	

Data set for these test were obtained from the airplane's flight manual, and for their respective test can be seen below as Table 7, Table 8 and Table 9.

Table 7: Diamond DV-20 engine performance test data set

Engine performance test	
Altitude	2000 ft / 6000 ft / 10000 ft

Table 8: Diamond DV-20 cruise performance test data set

Cruise performance test			
Altitude	RPM	MAP	
2000 ft	1900	24 inHg	55
	2200	25,7 inHg	75
	2260	26,7 inHg	95
6000 ft	2000	22 inHg	55
	2200	22,7 inHg	65
	2260	23,3 inHg	75
10000 ft	2200	19,7 inHg	55
	2260	20,3 inHg	65

Table 9: Diamond DV-20 climb performance test data set

Climb performance test				
Altitude	Low limit	High limit	Airspeed	Flaps
2000 ft	1650 ft	2350 ft	65 kn	TO
	1650 ft	2350 ft	70 kn	UP
6000 ft	5750 ft	6250 ft	63 kn	TO
	5750 ft	6250 ft	67 kn	UP
10000 ft	9850 ft	10150 ft	62 kn	TO
	9850 ft	10150 ft	65 kn	UP

Cruise performance test results are shown as $PIW \cdot VIW - VIW^4$ diagram in Figure 37, from which the following drag coefficients were obtained.

$$c_{D0} = 0,020254$$

$$c_{D2} = 0,060273$$

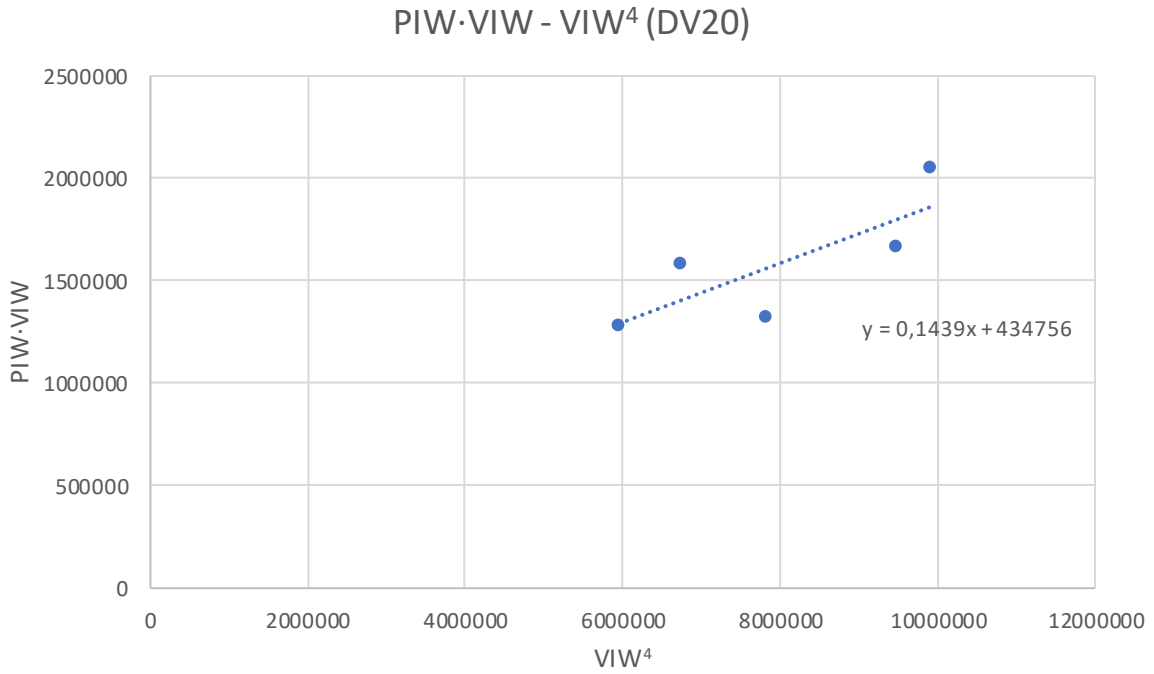


Figure 37: Cruise performance results for Diamond DV20

Climb performance results are shown as PIW – CIW diagram in Figure 38.

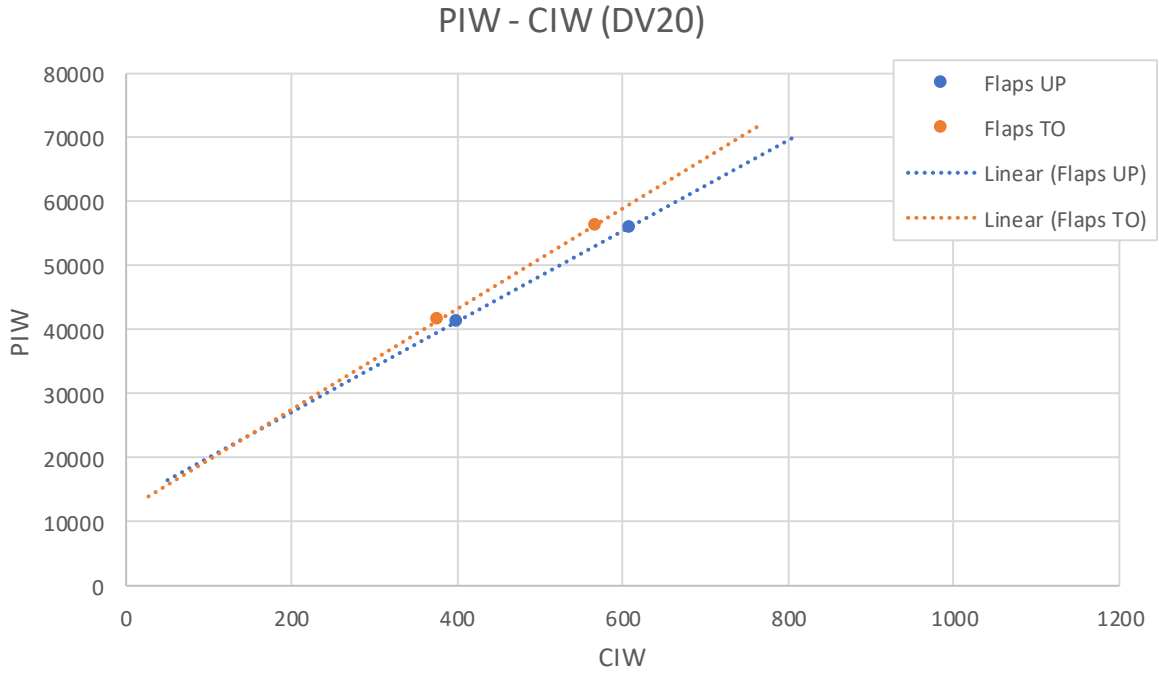


Figure 38: Climb performance results for Diamond DV20

6. Discussion

As a continuation on this project, the newly obtained improvements still require future updates, as new problems were and will be revealed in future modelling process.

An engine models are currently presenting the available engine power quite well, but they lack an input parameter. Their future updates should include a rpm limitation which would limit the maximum available power to the one available at a chosen rotational speed. This is useful when the modelled engines are combined with the fixed pitch propellers, which as we know limit the maximum engine rotational speed to the lower value that the one stated in engine specifications. This is a problem of both normally aspirated and pre-charged engines. One additional problem of pre-charged engine model is a slightly more complicated process of power modelling. As each engine can have different maximum manifold pressure and is different in construction, in terms of turbocharger or supercharger, which causes different response of engine above the critical altitude.

Propeller efficiency model for fixed pitch propeller is good but requires a lot of processing for the basic efficiency curve, this is a setback for the model. This will cause a certain requirement of calculation power, and with combination of multiple aircraft simulations, this process would be unachievable. For that is reason in future research the fixed pitch propeller model needs to be made more concise and more general, but with retention of the precision. Variable pitch propeller efficiency model was good, but now is confirmed through multiple calculations.

Drag coefficients are easy to determine, but with the impact they have on the overall performance model, it is very difficult to determine the correct drag polar. As seen earlier the drag polar for the Cessna 182 is symmetric and provides good drag coefficient for the performance model. In case of Cessna 206 the symmetric drag polar provides the better fit to the cruise data, but then the climb data has an offset which is quite big and causes a certain error. While using the asymmetric polar causes a small error in cruise data, but the climb data is correct and doesn't have an error. A symmetric polar for this aircraft can be seen on Figure 39, on in it can be seen that a symmetric polar can't cover both climb and cruise data, while

the Figure 40 shows the asymmetric drag polar which provides the better fit with small deviation to the cruise data.

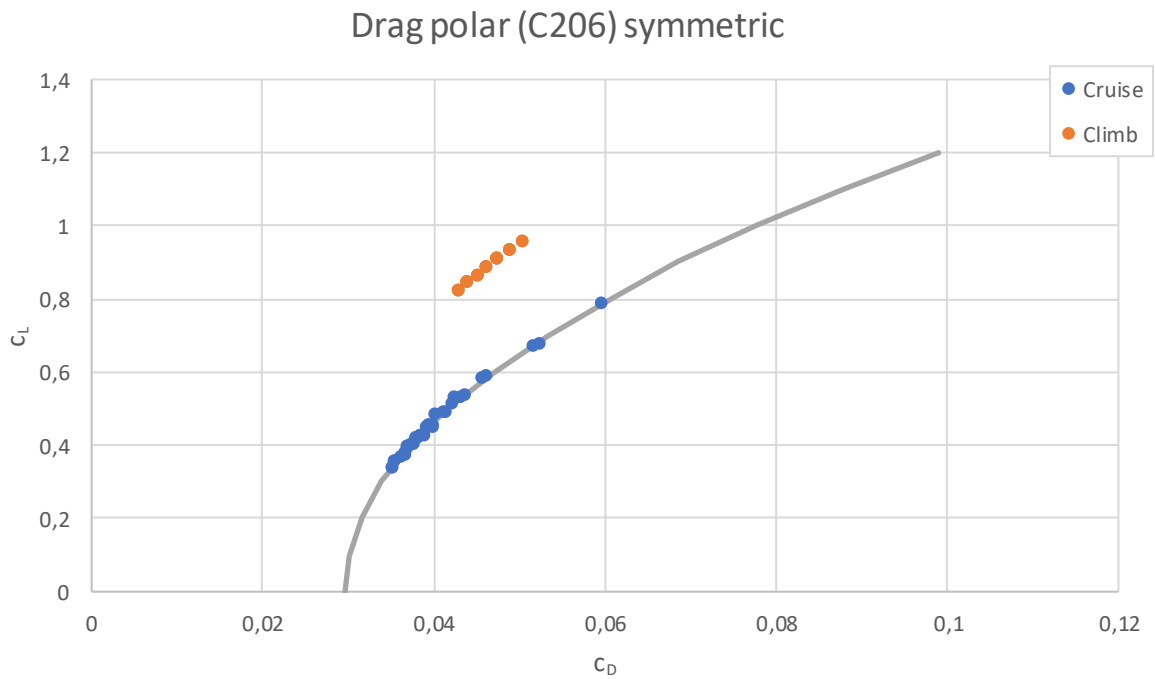


Figure 39: Symmetric drag polar for Cessna 206

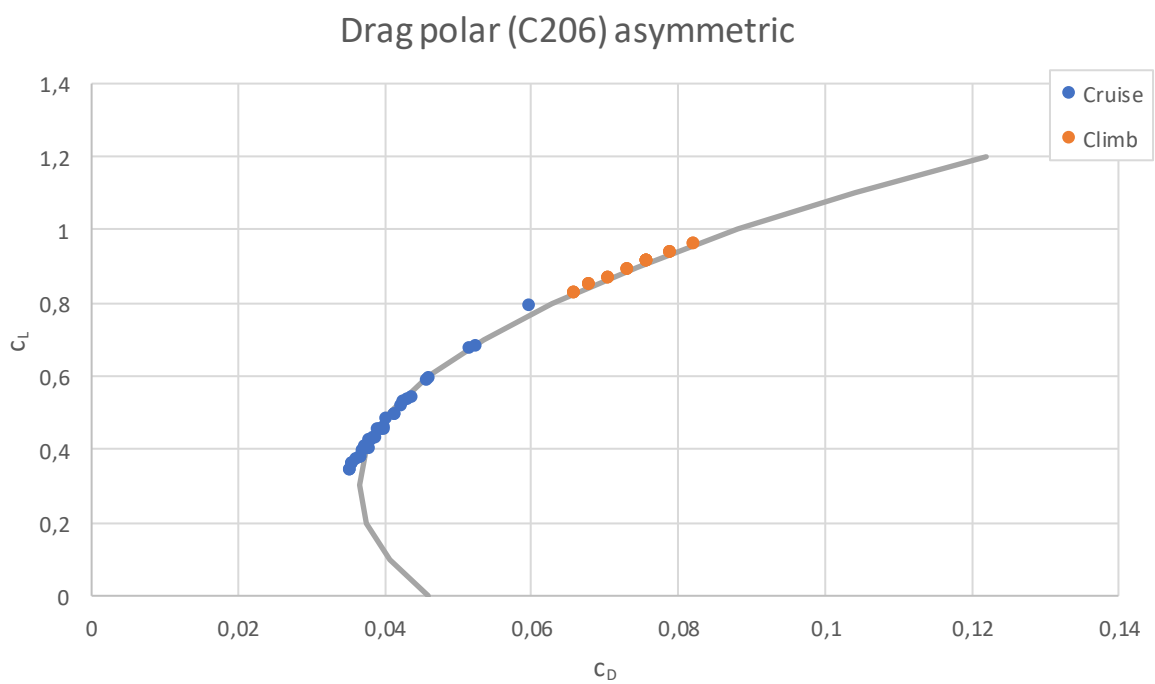


Figure 40: Asymmetric drag polar for Cessna 206

Vertical speed conversion is done quite simply and is necessary due to the way the data in aircraft's manual is obtained. Only possible problem that could present itself would be a different way of presenting the climb performance data in the aircraft's manual.

Throughout the whole research all the methods mentioned were used on multiple airplanes from different manufacturers. Some aircraft worked on are:

- Diamond DV20
- Cessna 162
- Cessna 172
- Cessna 182
- Cessna 182 TC
- Cessna 206
- Cessna 206 TC
- Cirrus SR22
- Piper 28
- Piper 44

Although the result would vary from one aircraft to the other, and one manufacturer to the other, some were consistent in improving the results. Some aircraft manuals were formatted better and contained more useful information, while the others were a real challenge to read and some even lacked crucial data. For that reason, work was more focused on certain manufacturers and certain aircraft types. Some of the aircraft revealed some issues that need to be overcome in future research and some should be used as an example for possible standardization of published aircraft data. Example of these problems are data points grouping in certain way that cannot be explained at his time for Piper 44 aircraft, and other would be Piper 28 which provides old and not updated aircraft manuals with very low precision performance charts.

Engine manuals used for engine power modelling were collected from different manufacturers, and while they served good purpose for modelling the engine power, some of them are not user-friendly and do not contain necessary data for other research such as flight tests. An example of this would be Rotax 912 S engine which doesn't provide typical engine diagram with altitude characteristic. This created additional problems where the data collected in flight test could be marked as obsolete if not for additional power and fuel flow modelling.

All the data was processed in form of calculation tables, as the process could be easily modified, and the results would be visible straight away. The data and results were plotted using the same calculation tables, but presenting them would be a challenge as they are quite large.

7. Conclusion

All the found improvements impact the model in their own way and in their own aspect. Some improvements were worked on as they provided the necessary reference points in the model, while other were introduced to mitigate some known problems. In all segments of the proposed improvements, the improvements were agreed on and then tested on certain aircraft spectrum. Result would vary from the airplane to the airplane, but positive result, even on a single aircraft, would usually discover new sets of problems that up to that point were unknown. For that reason, a lot of work has been done, with a lot of work left for the future participants in the project.

As in this case starting from a certain point along in the project, it is much harder than starting fresh. Starting fresh offers the possibility to notice and work on problems as they show up throughout the project. Joining in on an already started project, it is much more difficult, due to the fact that some time is required to start observing the project in the same way the other participants do. With that said a lot of time of the traineeship was taken by catching up to the project.

Research and development is much more satisfying in regard to the end result, but sometimes it is hard to see advancement, because unlike other work, for a small advancement vast amount of time and effort is used.

Opportunity to work with amazing people in an amazing environment such as Eurocontrol, is a one that no one should refuse. Working on a project that is within your passion, with people who are one of the best in their respectable fields, and exchanging thoughts and ideas, is certainly a good recipe for ones career path.

Bibliography

- [1] "Eurocontrol," [Online]. Available: <https://www.eurocontrol.int>. [Accessed 05 09 2020].
- [2] "Wikipedia - Eurocontrol," [Online]. Available: <https://en.wikipedia.org/wiki/Eurocontrol>. [Accessed 07 09 2020].
- [3] Eurocontrol Experimental Centre, User Manual for the Base of Aircraft Data (BADA) Family 4, 2012.
- [4] "Wikipedia - International Standard Atmosphere," [Online]. Available: https://en.wikipedia.org/wiki/International_Standard_Atmosphere. [Accessed August 2020].
- [5] S. Gudmundsson, General aviation aircraft design: Applied methods and procedures, Oxford: Butterworth-Heinemann, 2014.
- [6] European Aviation Safety Agency, Certification Specifications CS-23, Amendment 2, 2010.
- [7] R. D. Kimberlin, Flight Testing of Fixed-Winged Aircraft, Knoxville: American Institute of Aeronautics and Astronautics, 2003.

List of Figures

Figure 1: Atmospheric temperature up to 15000 m	8
Figure 2: Atmospheric pressure up to 15000 m	9
Figure 3: Atmospheric density up to 15000 m.....	10
Figure 4: Climb Power - Altitude ISA graph for Cessna 182	20
Figure 5: Climb Power - Altitude ISA graph for Cessna 182 with efficiency correction.....	21
Figure 6: Climb Power - Altitude OAT -20 °C graph for Cessna 182.....	22
Figure 7: Climb Power - Altitude OAT -20 °C graph for Cessna 182 with efficiency correction	23
Figure 8: Climb Power - Altitude OAT +20 °C graph for Cessna 182	24
Figure 9: Climb Power - Altitude OAT +20 °C graph for Cessna 182 with efficiency correction	25
Figure 10: Power - Altitude graph for Continental O-240-D (C162)	29
Figure 11: Power - Altitude graph for Lycoming IO-540-AB1A5 (C182)	30
Figure 12: Power - Altitude graph for Rotax 912-S (DV20)	31
Figure 13: Power - Altitude graph for Lycoming TIO-540-AK1A (C182TC)	34
Figure 14: Power - Altitude graph for Lycoming TIO-540-AJ1A (C206TC)	35
Figure 15: Maximum thrust – Airspeed graph for Cessna 172.....	38
Figure 16: Propeller efficiency graph for Cessna 172	40
Figure 17: Propeller efficiency graph for Cessna 182	42
Figure 18: Polar for Cessna 182 with cruise and climb points	46
Figure 19: Linear regression of lift drag coefficient combination for Cessna 182	47
Figure 20: Linear regression of $PIW \cdot VIW \cdot VIW^4$ combination for Cessna 182	48
Figure 21: Vertical speed / Rate of Climb comparison at different altitudes and temperatures graph for Cessna 206	50
Figure 22: Climb Power - Altitude ISA graph for Cessna 182	52
Figure 23: Climb Power - Altitude ISA graph for Cessna 182 TC.....	52
Figure 24: Climb Power - Altitude OAT ISA graph for Cessna 182.....	54
Figure 25: Climb Power - Altitude OAT -20 °C graph for Cessna 182.....	54
Figure 26: Climb Power - Altitude OAT +20 °C graph for Cessna 182	55

Figure 27: Climb Power - Altitude OAT -20 °C graph for Cessna 182 without vertical speed conversion	56
Figure 28: Climb Power - Altitude OAT +20 °C graph for Cessna 182 without vertical speed conversion	56
Figure 29: Climb Power - Altitude OAT -20 °C graph for Cessna 182.....	57
Figure 30: Climb Power - Altitude OAT +20 °C graph for Cessna 182	57
Figure 31: Vertical speed - Altitude graph for Cessna 182.....	58
Figure 32: Power - True Airspeed OAT ISA graph for Cessna 182	59
Figure 33: Power - True Airspeed OAT -20 °C graph for Cessna 182	59
Figure 34: Power - True Airspeed OAT +20 °C graph for Cessna 182	60
Figure 35: Cruise performance results for Cessna 172.....	69
Figure 36: Climb performance results for Cessna 172.....	69
Figure 37: Cruise performance results for Diamond DV20	72
Figure 38: Climb performance results for Diamond DV20.....	72
Figure 39: Symmetric drag polar for Cessna 206	74
Figure 40: Asymmetric drag polar for Cessna 206	74

List of Tables

Table 1: Fixed pitch propeller efficiency for Cessna 172	40
Table 2: Cessna 172 flight test checklist.....	67
Table 3: Cessna 172 cruise performance test data set.....	67
Table 4: Cessna 172 climb performance test data set.....	68
Table 5: Cessna 172 descent performance test data set.....	68
Table 6: Diamond DV-20 flight test checklist.....	70
Table 7: Diamond DV-20 engine performance test data set.....	71
Table 8: Diamond DV-20 cruise performance test data set.....	71
Table 9: Diamond DV-20 climb performance test data set.....	71

List of Equations

Equation 1: Standard atmospheric temperature at MSL.....	7
Equation 2: Standard atmospheric pressure at MSL.....	7
Equation 3: Standard atmospheric density at MSL.....	7
Equation 4: Standard speed of sound at MSL.....	7
Equation 5: Average tropopause altitude.....	7
Equation 6: Adiabatic index of air.....	7
Equation 7: Specific gas constant for air.....	7
Equation 8: Gravitational acceleration.....	8
Equation 9: ISA temperature gradient below tropopause.....	8
Equation 10: Temperature for altitudes below tropopause.....	8
Equation 11: Temperature for altitudes at and above tropopause.....	8
Equation 12: Air pressure for altitudes below tropopause.....	9
Equation 13: Air pressure for altitudes at and above tropopause.....	9
Equation 14: Air density according to perfect gas law.....	9
Equation 15: Temperature ratio.....	10
Equation 16: Pressure ratio.....	10
Equation 17: Density ratio.....	10
Equation 18: Speed of sound.....	10
Equation 19: Calibrated to True airspeed conversion.....	11
Equation 20: True to Calibrated airspeed conversion.....	11
Equation 21: Mach number.....	11
Equation 22: True airspeed from Mach number.....	11
Equation 23: Dynamic pressure.....	12
Equation 24: Aircraft weight.....	14
Equation 25: Aerodynamic force.....	14
Equation 26: Aerodynamic coefficient.....	14
Equation 27: Aerodynamic lift coefficient.....	15
Equation 28: Aerodynamic drag coefficient.....	15
Equation 29: All engine power.....	16

Equation 30: Power coefficient	16
Equation 31: Throttle regulated power coefficient.....	16
Equation 32: Power coefficient below critical altitude	17
Equation 33: Power coefficient above critical altitude	17
Equation 34: Propeller efficiency.....	17
Equation 35: Propeller efficiency polynomial expression.....	17
Equation 36: Rate of climb / descent.....	18
Equation 37: Gagg and Ferrar engine performance model	27
Equation 38: Normally aspirated engine performance model.....	28
Equation 39: Pre-charged engine power model	33
Equation 40: Sigma critical in standard atmospheric conditions	33
Equation 41: Power model power factor	33
Equation 42: Thrust power.....	36
Equation 43: Thrust	36
Equation 44: Static thrust	38
Equation 45: Cruise thrust	38
Equation 46: Maximum efficiency point	39
Equation 47: Highest airspeed thrust	39
Equation 48: Fixed pitch propeller efficiency matrix.....	39
Equation 49: Fixed pitch propeller efficiency coefficients.....	39
Equation 50: Cubic spline thrust.....	39
Equation 51: Fixed pitch propeller efficiency	40
Equation 52: Variable pitch propeller efficiency.....	42
Equation 53: Drag coefficient.....	45
Equation 54: Lift coefficient	45
Equation 55: Drag lift relationship	45
Equation 56: Drag lift relationship	45
Equation 57: PIW factor	45
Equation 58: VIW factor.....	45
Equation 59: Parasitic drag coefficient	46
Equation 60: Induced drag coefficient	46
Equation 61: Symmetric drag polar	46

Equation 62: Asymmetric drag polar	46
Equation 63: Vertical speed / Rate of Climb conversion	50
Equation 64: VIW factor source	64
Equation 65: VIW factor	64
Equation 66: PIW factor source	65
Equation 67: PIW factor	65
Equation 68: PIW factor	65
Equation 69: CIW factor	65
Equation 70: Vertical speed from CIW	66
Equation 71: NIW factor	66
Equation 72: Variable pitch propeller efficiency.....	87
Equation 73: Variable pitch propeller efficiency polynomial expression.....	87

List of Labels

a	speed of sound	m/s
AR	aspect ratio	-
c	coefficient	-
CIW	climb speed factor	-
e	Oswald efficiency	-
F	force	N
g_0	gravitational acceleration	m/s ²
H	altitude	m
J	advance factor	-
k	slope coefficient	-
l	intercept value	-
M	Mach number	-
m	mass	kg
n	quantity	-
NIW	rotation speed factor	-
p	pressure	Pa
P	power / engine power	W
PIW	power factor	-
q	dynamic pressure	Pa
R	specific gas constant for air	J/kg·K
S	area	m ²
T	temperature	K
v	speed	m/s
VIW	speed factor	-
W	engine power	W
β_T	temperature lapse coefficient	K/m
δ	pressure ratio	-
η	efficiency	-

θ	temperature ratio	-
κ	adiabatic index for air	-
ρ	density	kg/m ³
σ	density ratio	-
φ	bank angle	° (degree)

Subscripts

0	standard (ISA/MSL)
C	cruise airspeed
CAS	calibrated airspeed
crit	critical altitude
D	drag
D0	parasite drag
Di	induced drag
eng	engine
G	gravitational
H	maximum airspeed
ISA	international standard atmosphere
L	lift
max	maximum value
MSL	mean sea level
p	pressure
P	power
prop	propeller
ref	reference
T	temperature
TAS	true airspeed
trop	tropopause
turbo	turbocharger
v	vertical

Appendix A

The propeller efficiency for variable pitch propellers is modelled through the momentum theory.

Equation 72: Variable pitch propeller efficiency

$$\eta = 2 \cdot \eta_{max} \left(1 + \left[1 + 2 \cdot \eta \frac{\dot{W}_P}{n_{eng}} \left\{ \sigma \cdot \rho_0 \cdot D_P^2 \frac{\pi}{4} v_{TAS}^3 \right\}^{-1} \right]^{\frac{1}{2}} \right)^{-1}$$

Equation 73: Variable pitch propeller efficiency polynomial expression

$$2 \frac{\dot{W}_P}{n_{eng}} (\sigma \cdot \rho_0 \cdot D_P^2 \cdot \pi \cdot v_{TAS}^3 \cdot \eta_{max})^{-1} \cdot \eta^3 + \eta - \eta_{max} = 0$$

To obtain the propeller efficiency the propeller efficiency polynomial expression can be solved in the following way. [3]

$$\eta^3 + \left(\frac{n_{eng}}{\dot{W}_P} \cdot \sigma \cdot \rho_0 \cdot D_P^2 \cdot \frac{\pi}{2} \cdot v_{TAS}^3 \cdot \eta_{max} \right) \eta - \left(\frac{n_{eng}}{\dot{W}_P} \cdot \sigma \cdot \rho_0 \cdot D_P^2 \cdot \frac{\pi}{2} \cdot v_{TAS}^3 \cdot \eta_{max}^2 \right) = 0$$

$$a_1 = 0$$

$$a_2 = \frac{n_{eng}}{\dot{W}_P} \cdot \sigma \cdot \rho_0 \cdot D_P^2 \cdot \frac{\pi}{2} \cdot v_{TAS}^3 \cdot \eta_{max}$$

$$a_3 = \frac{n_{eng}}{\dot{W}_P} \cdot \sigma \cdot \rho_0 \cdot D_P^2 \cdot \frac{\pi}{2} \cdot v_{TAS}^3 \cdot \eta_{max}^2$$

$$Q = \frac{3 \cdot a_2 - a_1^2}{9} = \frac{n_{eng}}{\dot{W}_P} \cdot \sigma \cdot \rho_0 \cdot D_P^2 \cdot \frac{\pi}{6} \cdot v_{TAS}^3 \cdot \eta_{max}$$

$$R = \frac{9 \cdot a_1 \cdot a_2 - 27 \cdot a_3 - 2 \cdot a_1^3}{54} = \frac{n_{eng}}{\dot{W}_P} \cdot \sigma \cdot \rho_0 \cdot D_P^2 \cdot \frac{\pi}{4} \cdot v_{TAS}^3 \cdot \eta_{max}^2$$

$$D = Q^3 + R^2$$

$$S = \sqrt[3]{R + \sqrt{D}}$$

$$T = \sqrt[3]{R - \sqrt{D}}$$

$$\eta = S + T - \frac{a_1}{3} = S + T$$



University of Zagreb
Faculty of Transport and Traffic Sciences
10000 Zagreb
Vukelićeva 4

DECLARATION OF ACADEMIC INTEGRITY AND CONSENT

I declare and confirm by my signature that this _____ graduate thesis
is an exclusive result of my own work based on my research and relies on published literature,
as can be seen by my notes and references.

I declare that no part of the thesis is written in an illegal manner,
nor is copied from unreferenced work, and does not infringe upon anyone's copyright.

I also declare that no part of the thesis was used for any other work in
any other higher education, scientific or educational institution.

I hereby confirm and give my consent for the publication of my _____ graduate thesis
titled **Modelling and Validation of BADA 4 Aircraft Piston Performance**

on the website and the repository of the Faculty of Transport and Traffic Sciences and
the Digital Academic Repository (DAR) at the National and University Library in Zagreb.

In Zagreb, 20 September 2020

Student:
Paproči Petar
(signature)